Appendix: Macroeconomic Drivers of Bond and Equity Risks

John Y. Campbell, Carolin Pflueger, and Luis M. Viceira[1]

This draft: May 2019

[1]Campbell: Department of Economics, Littauer Center, Harvard University, Cambridge MA 02138, USA, and NBER. Email john_campbell@harvard.edu. Pflueger: University of British Columbia, Vancouver BC V6T 1Z2, Canada, and NBER. Email carolin.pflueger@sauder.ubc.ca. Viceira: Harvard Business School, Boston MA 02163, and NBER. Email lviceira@hbs.edu. This paper was previously circulated under the title "Monetary Policy Drivers of Bond and Equity Risks". We thank Jules van Binsbergen, John Cochrane, Olivier Coibion, Gregory Duffee, Harald Uhlig, Martin Lettau, Francisco Palomino, Monika Piazzesi, Rossen Valkanov, Stanley Zin, four anonymous referees, and conference and seminar participants for helpful comments. We thank Jiri Knesl, Alex Zhu, and particularly Gianluca Rinaldi for able research assistance. This material is based upon work supported by Harvard Business School Research Funding and the PH&N Centre for Financial Research at UBC.

This document is a supplemental appendix to Campbell, Pflueger, and Viceira (2019). The contents of this appendix are as follows:

1. Section A provides additional empirical results in support of the assumed link between consumption and the output gap.
2. Section B derives the log-linear expansion for habit around the steady-state.
3. Section C derives the solution for the macroeconomic dynamics in a simplified special case and the full model.
4. Section D describes the model solution for both macroeconomic dynamics and asset pricing moments.
5. Section E describes in detail the implementation of the numerical model solution.
6. Section F provides details for the econometric methodology. Among other details, it describes how we estimate orthogonalized macroeconomic impulse responses.
7. Section G provides additional model results, in particular impulse responses when setting the new parameters θ_1 and θ_2 to zero.

A Additional empirical results

Figure A.1 shows that equation (2) in the main paper is a close description of consumption and output gap data. We regress stochastically detrended consumption onto the output gap:

$$\hat{c}_t = b_0 + b_x x_t + \varepsilon_t. \tag{A.1}$$

We set the smoothing parameter to $\phi = 0.93$ (half-life 2.4 years) to maximize the correlation between $\hat{c}_t$ and the output gap. Figure A.1 shows that $\hat{c}_t$ and its fitted value from (A.1) track each other through different macroeconomic regimes, with a correlation of 77%. The estimated slope coefficient b_x is statistically indistinguishable from one.

To test whether the functional form of equation (2) in the main paper is actually a good description of the data, we add inflation and the nominal Federal Funds rate as additional controls to (A.1). We find that neither of these variables enter in a statistically or economically significant manner.

Specifically, our regression results are as follows. "Fitted (Output)" is the fitted value from the quarterly regression $\hat{c}_t = \underset{(0.27)}{11.73} + \underset{(0.17)}{0.88} x_t + \varepsilon_t$; "Fitted (Output, Inflation)" is the fitted value from the quarterly regression $\hat{c}_t = \underset{(0.45)}{11.72} + \underset{(0.17)}{0.88} x_t + \underset{(0.12)}{0.00} \pi_t + \varepsilon_t$;

Figure A.1: Stochastically Detrended Consumption vs. Output Gap

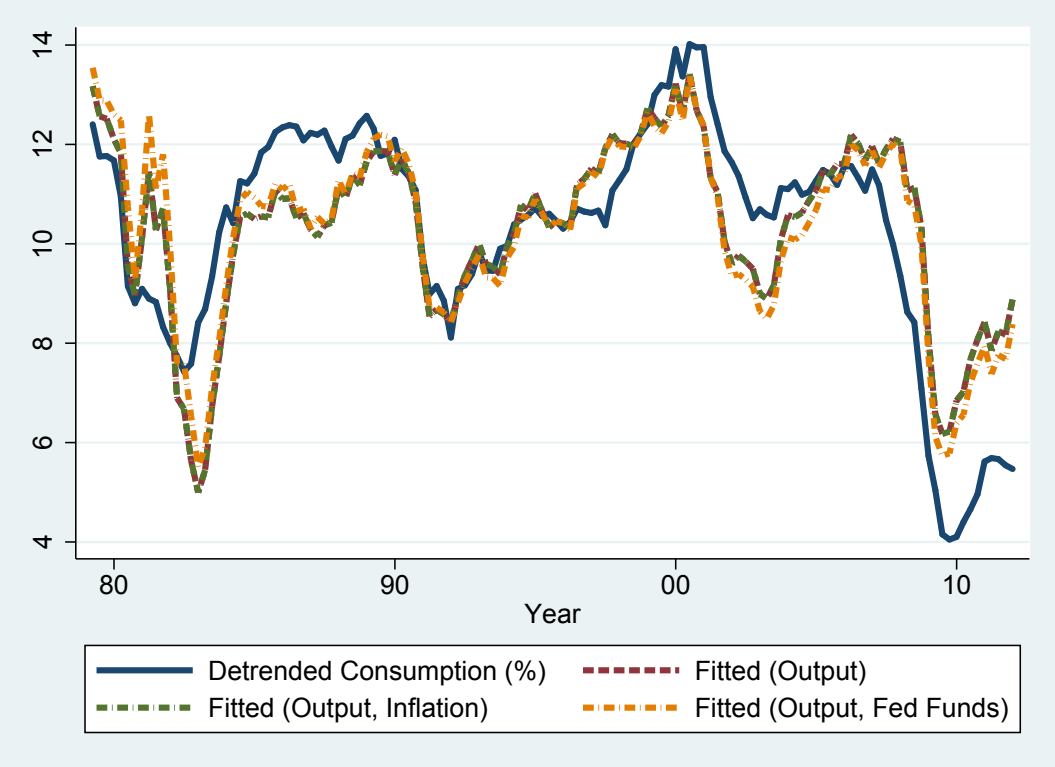

This figure plots the time series of stochastically exponentially detrended consumption $\hat{c}_t = c_t - (1-\phi)[c_{t-1} + \phi c_{t-2} + ...]$. The smoothing parameter $\phi = 0.93$, corresponding to a half-life of 2.4 years, is chosen to maximize the univariate correlation between the log real output gap and exponentially detrended consumption. "Fitted(Output)" is the fitted value from the quarterly regression $\hat{c}_t = \underset{(0.27)}{11.73} + \underset{(0.17)}{0.88}\, x_t + \varepsilon_t$; "Fitted(Output, Inflation)" is the fitted value from the quarterly regression $\hat{c}_t = \underset{(0.45)}{11.72} + \underset{(0.17)}{0.88}\, x_t + \underset{(0.12)}{0.00}\, \pi_t + \varepsilon_t$; "Fitted(Output, Fed Funds)" is the fitted value from the quarterly regression $\hat{c}_t = \underset{(0.54}{11.16} + \underset{(0.14)}{0.86}\, x_t + \underset{(0.08)}{0.09}\, i_t + \varepsilon_t$. All regressions use the full sample 1979Q3-2011Q4 and show Newey-West standard errors with four lags in parentheses. Data for consumption, the output gap, inflation, and the Federal Funds rate are as described in section 4.1 in the main paper.

"Fitted (Output, Fed Funds)" is the fitted value from the quarterly regression $\hat{c}_t = \underset{(0.54}{11.16} + \underset{(0.14)}{0.86} x_t + \underset{(0.08)}{0.09} i_t + \varepsilon_t$. Newey-West standard errors with four lags are shown in parentheses and all regressions are for the full sample 1979Q3-2011Q4.

B Loglinear habit dynamics around steady state

This section derives the loglinear dynamics of the habit stock. We use a first order approximation around the steady state $S_t = \bar{S}$ to write log habit h_t as a linear

function in $c_t, c_{t-1}, ...$ and $E_t\Delta c_{t+1}, E_{t-1}\Delta c_t, ...$ Equation (8) in the paper models how habit adjusts to consumption implicitly by modeling the evolution of the log surplus consumption ratio. In order to solve for log habit we need an approximate relation between log habit, log consumption, and the log surplus consumption ratio.

Defining $\hat{s}_t = s_t - \bar{s}$, we develop a first-order Taylor expansion of $\hat{s}_t$ in terms of $c_t - h_t$. We take the first derivative of $\hat{s}_t$ with respect to $c_t - h_t$:

$$\begin{aligned}
\frac{d\hat{s}_t}{d(c_t - h_t)} &= \frac{d}{d(c_t - h_t)}\left(\log\left(\frac{1 - exp(-(c_t - h_t))}{\bar{S}}\right)\right), && \text{(B.1)}\\
&= \frac{\bar{S}}{1 - exp(-(c_t - h_t))}\frac{exp(-(c_t - h_t))}{\bar{S}}, && \text{(B.2)}\\
&= -\left(1 - \frac{1}{S_t}\right), && \text{(B.3)}
\end{aligned}$$

so at the steady state this first derivative equals:

$$\left.\frac{d\hat{s}_t}{d(c_t - h_t)}\right|_{S_t = \bar{S}} = -\left(1 - \frac{1}{\bar{S}}\right). \quad \text{(B.4)}$$

The first order Taylor expansion for $\hat{s}_t$ in terms of $c_t - h_t$ around the steady-state therefore equals (up to constant):

$$\hat{s}_t \approx \left(1 - \frac{1}{\bar{S}}\right)(h_t - c_t), \quad \text{(B.5)}$$

or

$$h_t \approx c_t + \frac{\hat{s}_t}{1 - \frac{1}{\bar{S}}}. \quad \text{(B.6)}$$

6

The relation (B.6) is approximate rather than exact because we ignore second- and higher-order terms in $(c_t - h_t)$.

Because $\lambda(\bar{s}) = \frac{1}{\bar{S}} - 1$ and the dynamics for log surplus consumption are given by equation (8) in the main paper, the approximate dynamics for $\hat{s}_t$ near the steady state are given by:

$$\hat{s}_{t+1} \approx \theta_0\hat{s}_t + \theta_1 x_t + \theta_2 x_{t-1} + \left(\frac{1}{\bar{S}} - 1\right)\varepsilon_{c,t+1}. \quad \text{(B.7)}$$

Equation (B.7) is approximate rather than exact because we have replaced the exact sensitivity function $\lambda(s_t)$ by its steady state value $\lambda(\bar{s}) = \frac{1}{\bar{S}} - 1$.

Combining (B.6) with (B.7) gives the approximate dynamics for log habit:

$$h_{t+1} \approx c_{t+1} + \frac{1}{1-\frac{1}{\bar{S}}}\hat{s}_{t+1}, \tag{B.8}$$

$$\approx c_{t+1} + \frac{1}{1-\frac{1}{\bar{S}}}\left(\theta_0\hat{s}_t + \theta_1 x_t + \theta_2 x_{t-1} + \left(\frac{1}{\bar{S}} - 1\right)\varepsilon_{c,t+1}\right), \tag{B.9}$$

$$\approx c_{t+1} - \varepsilon_{c,t+1} + \theta_0\left(h_t - c_t\right) + \frac{\theta_1}{1-\frac{1}{\bar{S}}}x_t + \frac{\theta_2}{1-\frac{1}{\bar{S}}}x_{t-1}, \tag{B.10}$$

$$\approx \theta_0 h_t + (1-\theta_0)c_t + \mathrm{E}_t\Delta c_{t+1} - \frac{\theta_1 x_t + \theta_2 x_{t-1}}{\frac{1}{\bar{S}} - 1}, \tag{B.11}$$

where we use $\Delta c_{t+1} = c_{t+1} - c_t$ to denote the change in log consumption from time t to time $t+1$. We now iterate (B.11) to obtain:

$$h_{t+1} \approx \sum_{j=0}^{\infty}\theta_0^j\left((1-\theta_0)c_{t-j} + E_{t-j}\Delta c_{t-j+1} - \frac{\theta_1 x_{t-j} + \theta_2 x_{t-j-1}}{\frac{1}{\bar{S}} - 1}\right), \tag{B.12}$$

$$\approx (1-\theta_0)\sum_{j=0}^{\infty}\theta_0^j c_{t-j} + \sum_{j=0}^{\infty}\theta_0^j E_{t-j}\Delta c_{t-j+1} - \frac{\theta_1}{\frac{1}{\bar{S}} - 1}x_t \tag{B.13}$$

$$-\frac{\theta_0\theta_1 + \theta_2}{\frac{1}{\bar{S}} - 1}\sum_{j=0}^{\infty}\theta_0^j x_{t-j-1}. \tag{B.14}$$

Substituting in for x_t from equation (2) in the main paper expresses habit in terms of lags of consumption and lags of expected consumption growth:

$$h_{t+1} \approx (1-\theta_0)\sum_{j=0}^{\infty}\theta_0^j c_{t-j} + \sum_{j=0}^{\infty}\theta_0^j E_{t-j}\Delta c_{t-j+1} \tag{B.15}$$

$$-\frac{\theta_1}{\frac{1}{\bar{S}} - 1}\left(c_t - (1-\phi)\sum_{i=0}^{\infty}\phi^i c_{t-1-i}\right) \tag{B.16}$$

$$-\frac{\theta_0\theta_1 + \theta_2}{\frac{1}{\bar{S}} - 1}\sum_{j=0}^{\infty}\theta_0^j\left(c_{t-j-1} - (1-\phi)\sum_{i=0}^{\infty}\phi^i c_{t-j-2-i}\right). \tag{B.17}$$

When $\theta_1 = \theta_2 = 0$ (the Campbell-Cochrane case), expression (B.17) shows that log habit is approximately an exponentially-weighted moving average of lagged log consumption and lagged consumption growth expectations. If expected consumption growth is constant, as is the case in Campbell and Cochrane (1999), the expected consumption growth terms drop out and the approximate habit dynamics are simply an exponentially-weighted moving average of lagged consumption.

Because $\frac{1}{\frac{1}{\bar{S}}-1} > 0$ and $1-\phi$ is close to zero, a negative value for θ_1 increases the dependence of habit on the first and second lags of consumption, while a positive value for θ_2 decreases the dependence on the second lag of consumption. Our calibration has $-\theta_1 > 0$, and $\theta_1(1-\phi) - (\theta_0\theta_1 + \theta_2) > 0$. Equation (B.17) then implies that habit loads more on the first and second lags of consumption compared to the Campbell-Cochrane case.

C Derivation of the macroeconomic solution

This appendix describes how we solve for the equilibrium dynamics of the output gap. Our goal is not to present the most general solution method or to provide an innovative solution. To make this clear, we have switched to solving the model via the standard Blanchard and Kahn (1980) methodology for rational expectations models. We previously used the generalized eigenvector method of Uhlig (1999) to solve for macroeconomic dynamics. Switching to the Blanchard and Kahn (1980) method leaves all our numerical model moments unchanged.

We are clear about the fact that we encounter the issue of multiple equilibria and we do not resolve this issue. Instead, we pick one equilibrium from those with the minimum number of lagged state variables and without sunspots. Our goal is to understand the asset pricing implications of consumption-based habit formation preferences with different macroeconomic dynamics and we think that this central point is not specific to a selected equilibrium.

To clarify our solution methodology we look at a particularly simple special case, where the simple analytic expressions can be found via the method of undetermined coefficients. The main difference in the solution technique for the full model is that a simple analytic expression for the lead-lag coefficients is no longer available. We therefore use the standard Blanchard and Kahn (1980) method to solve for the lead-lag coefficients. Both the special case and the full model have analytic expressions for the output gap innovation.

One important question is whether VAR(1) equilibrium dynamics for the output gap can be consistent with the loglinear macroeconomic Euler equation, which contains two lags of the output gap. Both in the special case and in the full model, we demonstrate that our solution for the lag coefficients and the output gap innovation takes exactly the form required to be consistent with the loglinear macro Euler equation (equation (17) in the main paper).

C.1 Simplified special case

We consider a special case, that has a particularly simple solution. We make the following two simplifying assumptions:

$$\pi_t = 0, \tag{C.1}$$

$$i_t = v_t, \tag{C.2}$$

where v_t is an iid shock. To simplify the algebra, inflation is assumed to equal zero and the nominal interest rate follows an iid process. This is a special case of the VAR(1) dynamics for inflation and the nominal short rate assumed in the paper.

Substituting the Fisher equation $r_t = i_t - E_t\pi_{t+1}$ into equation (17) in the main paper shows that the output gap satisfies the forward- and backward-looking Euler equation:

$$x_t = \frac{1}{\phi - \theta_1} E_t x_{t+1} + \frac{\theta_2}{\phi - \theta_1} x_{t-1} - \frac{1}{\gamma(\phi - \theta_1)}(i_t - E_t\pi_{t+1}). \tag{C.3}$$

Plugging in the simplifying assumptions (C.1) and (C.2) turns the Euler equation into:

$$x_t = \frac{1}{\phi - \theta_1} E_t x_{t+1} + \frac{\theta_2}{\phi - \theta_1} x_{t-1} - \frac{1}{\gamma(\phi - \theta_1)} v_t. \tag{C.4}$$

C.1.1 Method of undetermined coefficients

For the special case, we can solve the model via the method of undetermined coefficients. We start by guessing that the output gap follows the AR(1) dynamics:

$$x_t = b_{xx} x_{t-1} + u_{x,t}, \tag{C.5}$$

where b_{xx} is an unknown constant and $u_{x,t}$ is an iid shock. Equation (C.5) is the natural analogue to equation (25) in the main paper for the special case (C.1) and (C.2).

Substituting the guess (C.5) into the Euler equation (C.4) gives:

$$x_t = \frac{1}{\phi - \theta_1} b_{xx} x_t + \frac{\theta_2}{\phi - \theta_1} x_{t-1} - \frac{1}{\gamma(\phi - \theta_1)} v_t. \tag{C.6}$$

Re-arranging (C.6) gives:

$$x_t = \frac{\theta_2}{\phi - \theta_1 - b_{xx}} x_{t-1} - \frac{1}{\gamma(\phi - \theta_1 - b_{xx})} v_t. \tag{C.7}$$

Comparing (C.7) and (C.5) shows that there is a solution of the form (C.5) provided that we can find a coefficient b_{xx} such that:

$$b_{xx} = \frac{\theta_2}{\phi - \theta_1 - b_{xx}}. \tag{C.8}$$

Equivalently, b_{xx} must satisfy the quadratic equation:

$$b_{xx}^2 + b_{xx}(\theta_1 - \phi) + \theta_2 = 0. \tag{C.9}$$

Because the quadratic equation (C.9) may have zero, one, or two real-valued solutions, there may or may not exist a real-valued solution of the form (C.5). If a real solution for b_{xx} exists, it is given by:

$$b_{xx} = -\frac{\theta_1 - \phi}{2} \pm \sqrt{\left(\frac{\theta_1 - \phi}{2}\right)^2 - \theta_2}. \tag{C.10}$$

From now on we assume that $\left(\frac{\theta_1-\phi}{2}\right)^2-\theta_2 \geq 0$, so there exists a real-valued solution of the form (C.5). This is consistent with our treatment in the paper, where we exclude regions of the parameter space, where there is no real-valued VAR(1) solution. When there exists a real-valued solution for b_{xx}, there may exist more than one. For the current argument, it does not matter which one we pick. So, let's say that we have a procedure in place that picks one solution for b_{xx}.

We next obtain an analytic expression for the output gap innovation $u_{x,t} \equiv x_t - E_{t-1}x_t$ in terms of the shock v_t. Comparing (C.7) and (C.5) shows that for a given coefficient b_{xx} the output gap innovation equals:

$$u_{x,t} = -\frac{1}{\gamma(\phi-\theta_1-b_{xx})}v_t. \tag{C.11}$$

C.1.2 Consistency with macroeconomic Euler Equation

The analytic solution in the special case clarifies why there may exist an AR(1) solution for the output gap, even though the Euler equation contains two lags. To understand the apparent inconsistency, write the Euler equation (C.3) in the form:

$$x_t = (\phi-\theta_1)x_{t-1}-\theta_2 x_{t-2}+\frac{1}{\gamma}\left(i_{t-1}-E_{t-1}\pi_t\right)+u_{x,t}, \tag{C.12}$$

where $u_{x,t}$ is defined as $u_{x,t} \equiv x_t - E_{t-1}x_t$. With the simplifying assumptions (C.1) and (C.2) this becomes:

$$x_t = (\phi-\theta_1)x_{t-1}-\theta_2 x_{t-2}+\frac{1}{\gamma}v_{t-1}+u_{x,t}. \tag{C.13}$$

The apparent inconsistency arises because equation (C.13) has two lags of the output gap whereas (C.5) has only one.

In the special case, it straightforward to see that (C.13) is satisfied. With the output gap shock given by (C.11), the linear combination of x_{t-2} and v_{t-1} that appears on the right-hand-side of (C.13) is a multiple of x_{t-1}:

$$\begin{aligned} & -\theta_2 x_{t-2}+\frac{1}{\gamma}v_{t-1}, && \text{(C.14)}\\ = \; & -\theta_2 x_{t-2}-(\phi-\theta_1-b_{xx})\,u_{x,t-1}, && \text{(C.15)}\\ = \; & -(\phi-\theta_1-b_{xx})\left(b_{xx}x_{t-2}+u_{x,t-1}\right), && \text{(C.16)}\\ = \; & -(\phi-\theta_1-b_{xx})x_{t-1}. && \text{(C.17)} \end{aligned}$$

Substituting (C.17) into (C.13), the right-hand-side of (C.13) has only one lag and equals $b_{xx}x_{t-1}+u_{x,t-1}$.

C.2 Full model

We now solve the full model. Subsection C.2.1 recaps the macroeconomic side of the full model. Subsection C.2.2 shows that there exists a VAR(1) solution for the output gap if we can solve a set of three coupled quadratic equations. It also derives an analytic expression for the output gap shock, $u_{x,t}$. Subsection C.2.3 uses the analytic expressions derived in the previous section to show consistency with the loglinear macroeconomic Euler equation. Subsection C.2.4 states and applies Blanchard-Kahn to find the coefficients in the VAR(1) output gap dynamics. Finally, subsection C.2.4 replicates the proof of Blanchard-Kahn and extends it to show that the same algebra continues to give a (non-unique) solution when the system has fewer eigenvalues outside the unit circle than non-predetermined variables.

C.2.1 Model summary

We recap the macroeconomic side of the full model. Define the inflation and interest rate gaps relative to the random walk component in inflation:

$$\begin{aligned} \hat{\pi}_t &= \pi_t - \pi_t^*, && \text{(C.18)} \\ \hat{i}_t &= i_t - \pi_t^*. && \text{(C.19)} \end{aligned}$$

The exogenously given dynamics for inflation and the short-term nominal interest rate are:

$$\begin{aligned} \hat{\pi}_t &= b_{\pi x} x_{t-1} + b_{\pi\pi}\hat{\pi}_{t-1} + b_{\pi i}\hat{i}_{t-1} + v_{\pi,t}, && \text{(C.20)} \\ \hat{i}_t &= b_{ix} x_{t-1} + b_{i\pi}\hat{\pi}_{t-1} + b_{ix}\hat{i}_{t-1} + v_{i,t}, && \text{(C.21)} \\ \pi_t^* &= \pi_{t-1}^* + v_t^*. && \text{(C.22)} \end{aligned}$$

The output gap satisfies the Euler equation (C.3), which can be re-written in terms of $\hat{\pi}$ and $\hat{i}$ as

$$x_t = \frac{1}{\phi - \theta_1} E_t x_{t+1} + \frac{\theta_2}{\phi - \theta_1} x_{t-1} - \frac{1}{\gamma(\phi - \theta_1)} \left(\hat{i}_t - E_t \hat{\pi}_{t+1} \right). \quad \text{(C.23)}$$

Recall that we want to find a solution of the form

$$\hat{Y}_t = B\hat{Y}_{t-1} + \Sigma v_t, \quad \text{(C.24)}$$

where

$$\hat{Y}_t = \left[x_t, \hat{\pi}_t, \hat{i}_t \right]'. \quad \text{(C.25)}$$

We do not claim that these are the only possible solution dynamics, and other solutions may exist.

C.2.2 Method of undetermined coefficients

We now show that a solution of the form (C.24) exists if we can solve a set of three coupled quadratic equations, and derive an analytic expression for the output gap shock $u_{x,t}$. Equations (C.20) and (C.21) are already in the desired form, so we only need to solve for b_{xx}, $b_{x\pi}$, and b_{xi} (the first row of the matrix B). We guess a solution of the form:

$$x_t = b_{xx}x_{t-1} + b_{x\pi}\hat{\pi}_{t-1} + b_{xi}\hat{\hat{i}}_{t-1} + u_{x,t}. \tag{C.26}$$

We then substitute the guess (C.26) into the Euler equation (C.23) to find that:

$$\begin{aligned} x_t &= \frac{1}{\phi-\theta_1}\left[b_{xx}x_t + b_{x\pi}\hat{\pi}_t + b_{xi}\hat{\hat{i}}_t\right] + \frac{\theta_2}{\phi-\theta_1}x_{t-1} \\ &\quad -\frac{1}{\gamma(\phi-\theta_1)}\left(\hat{\hat{i}}_t - \left[b_{\pi x}x_t + b_{\pi\pi}\hat{\pi}_t + b_{\pi i}\hat{\hat{i}}_t\right]\right). \end{aligned} \tag{C.27}$$

Re-arranging to isolate x_t:

$$\begin{aligned} \left(1 - \frac{b_{xx}}{\phi-\theta_1} - \frac{b_{\pi x}}{\gamma(\phi-\theta_1)}\right)x_t &= \left(\frac{b_{x\pi}}{\phi-\theta_1} + \frac{b_{\pi\pi}}{\gamma(\phi-\theta_1)}\right)\hat{\pi}_t \\ &\quad + \left(\frac{b_{xi}}{\phi-\theta_1} + \frac{b_{\pi i}-1}{\gamma(\phi-\theta_1)}\right)\hat{\hat{i}}_t \\ &\quad + \frac{\theta_2}{\phi-\theta_1}x_{t-1}. \end{aligned} \tag{C.28}$$

We next substitute in (C.20) and (C.21) and divide by $1 - \frac{b_{xx}}{\phi-\theta_1} - \frac{b_{\pi x}}{\gamma(\phi-\theta_1)}$ to re-write condition (C.28) as:

$$\begin{aligned} x_t &= \frac{b_{x\pi} + \frac{b_{\pi\pi}}{\gamma}}{\phi-\theta_1-b_{xx}-\frac{b_{\pi x}}{\gamma}}\left[b_{\pi x}x_{t-1} + b_{\pi\pi}\hat{\pi}_{t-1} + b_{\pi i}\hat{\hat{i}}_{t-1} + v_{\pi,t}\right] \\ &\quad + \frac{b_{xi} + \frac{b_{\pi i}-1}{\gamma}}{\phi-\theta_1-b_{xx}-\frac{b_{\pi x}}{\gamma}}\left[b_{ix}x_{t-1} + b_{i\pi}\hat{\pi}_{t-1} + b_{ii}\hat{\hat{i}}_{t-1} + v_{i,t}\right] \\ &\quad + \frac{\theta_2}{\phi-\theta_1-b_{xx}-\frac{b_{\pi x}}{\gamma}}x_{t-1}. \end{aligned} \tag{C.29}$$

We re-arrange the right-hand side of (C.29) in the form of a VAR(1) equation:

$$\begin{aligned} x_t &= \frac{\left(b_{x\pi}+\frac{b_{\pi\pi}}{\gamma}\right)b_{\pi x}+\left(b_{xi}+\frac{b_{\pi i}-1}{\gamma}\right)b_{ix}+\theta_2}{\phi-\theta_1-b_{xx}-\frac{b_{\pi x}}{\gamma}}x_{t-1} \\ &+\frac{\left(b_{x\pi}+\frac{b_{\pi\pi}}{\gamma}\right)b_{\pi\pi}+\left(b_{xi}+\frac{b_{\pi i}-1}{\gamma}\right)b_{i\pi}}{\phi-\theta_1-b_{xx}-\frac{b_{\pi x}}{\gamma}}\hat{\pi}_{t-1} \\ &+\frac{\left(b_{x\pi}+\frac{b_{\pi\pi}}{\gamma}\right)b_{\pi i}+\left(b_{xi}+\frac{b_{\pi i}-1}{\gamma}\right)b_{ii}}{\phi-\theta_1-b_{xx}-\frac{b_{\pi x}}{\gamma}}\hat{i}_{t-1} \\ &+\frac{b_{x\pi}+\frac{b_{\pi\pi}}{\gamma}}{\phi-\theta_1-b_{xx}-\frac{b_{\pi x}}{\gamma}}v_{\pi,t}+\frac{b_{xi}+\frac{b_{\pi i}-1}{\gamma}}{\phi-\theta_1-b_{xx}-\frac{b_{\pi x}}{\gamma}}v_{i,t}. \end{aligned} \tag{C.30}$$

Equation (C.30) shows that there exists a solution of the form (C.26) if we can find coefficients b_{xx}, $b_{x\pi}$, and b_{xi} such that:

$$b_{xx} = \frac{\left(b_{x\pi}+\frac{b_{\pi\pi}}{\gamma}\right)b_{\pi x}+\left(b_{xi}+\frac{b_{\pi i}-1}{\gamma}\right)b_{ix}+\theta_2}{\phi-\theta_1-b_{xx}-\frac{b_{\pi x}}{\gamma}}, \tag{C.31}$$

$$b_{x\pi} = \frac{\left(b_{x\pi}+\frac{b_{\pi\pi}}{\gamma}\right)b_{\pi\pi}+\left(b_{xi}+\frac{b_{\pi i}-1}{\gamma}\right)b_{i\pi}}{\phi-\theta_1-b_{xx}-\frac{b_{\pi x}}{\gamma}}, \tag{C.32}$$

$$b_{xi} = \frac{\left(b_{x\pi}+\frac{b_{\pi\pi}}{\gamma}\right)b_{\pi i}+\left(b_{xi}+\frac{b_{\pi i}-1}{\gamma}\right)b_{ii}}{\phi-\theta_1-b_{xx}-\frac{b_{\pi x}}{\gamma}}. \tag{C.33}$$

Equation (C.30) gives an analytical expression for the output gap innovation $u_{x,t} \equiv x_t - E_{t-1}x_t$ in terms of the shocks $v_{\pi,t}$ and $v_{i,t}$ and the solution coefficients b_{xx}, $b_{x\pi}$, and b_{xi}:

$$u_{x,t} = \frac{b_{x\pi}+\frac{b_{\pi\pi}}{\gamma}}{\phi-\theta_1-b_{xx}-\frac{b_{\pi x}}{\gamma}}v_{\pi,t}+\frac{b_{xi}+\frac{b_{\pi i}-1}{\gamma}}{\phi-\theta_1-b_{xx}-\frac{b_{\pi x}}{\gamma}}v_{i,t}. \tag{C.34}$$

One might be concerned that the deterministic relation between $u_{x,t}$, $v_{\pi,t}$, and $u_{i,t}$ in equation (C.34) generates a singular variance-covariance matrix that would be trivial to reject in the data. However, our observable variables are π_t and i_t, whereas the gap variables $\hat{\pi}_t$ and $\hat{i}_t$ are unobservable. The shock to the random walk component of inflation, v_t^*, ensures that the variance-covariance matrix for the observable variables x_t, π_t, and i_t is non-singular at our point estimates for periods 1 and 2.

C.2.3 Consistency with macroeconomic Euler equation

By construction, a solution satisfying equations (C.31) through (C.33) and (C.34) must satisfy the Euler equation (C.23). In addition, this subsection shows explicitly

that the loglinear macroeconomic Euler equation is satisfied. From now on we assume that we are in a portion of the parameter space where the coupled quadratic equations (C.31) through (C.33) have at least one solution and we have picked one solution.

To see the apparent inconsistency, we use that $E_t x_{t+1} = x_{t+1} - u_{x,t+1}$ and substitute the inflation and interest rate dynamics (C.20) and (C.21) into the Euler equation (C.23):

$$x_t = \left(\phi - \theta_1 - \frac{b_{\pi x}}{\gamma}\right) x_{t-1} - \theta_2 x_{t-2} - \left(\frac{b_{\pi\pi}}{\gamma}\right) \hat{\pi}_{t-1} + \left(\frac{1}{\gamma} - \frac{b_{\pi i}}{\gamma}\right) \hat{i}_{t-1} + u_{x,t}, \tag{C.35}$$

where $u_{x,t}$ is defined as $u_{x,t} = x_t - E_{t-1} x_t$. Equation (C.35) has two lags of the output gap, whereas (C.26) has only one, so the two equations might appear inconsistent.

However, if b_{xx}, $b_{x\pi}$, and b_{xi} are such (C.31) through (C.33) hold and $u_{x,t}$ is given by (C.34), it is straightforward to see that there is no inconsistency. We know that under these conditions (C.27) holds in every state. A simple re-arrangement of (C.27) and shifting $t \to t-1$ shows that it is equivalent to:

$$\begin{aligned} &\left(\phi - \theta_1 - \frac{b_{\pi x}}{\gamma}\right) x_{t-1} - \theta_2 x_{t-2} - \left(\frac{b_{\pi\pi}}{\gamma}\right) \hat{\pi}_{t-1} + \left(\frac{1}{\gamma} - \frac{b_{\pi i}}{\gamma}\right) \hat{i}_{t-1} \\ = \;& b_{xx} x_{t-1} + b_{x\pi} \hat{\pi}_{t-1} + b_{xi} \hat{i}_{t-1}. \end{aligned} \tag{C.36}$$

Substituting this into the right-hand-side of (C.35) shows that it equals $b_{xx} x_{t-1} + b_{x\pi} \hat{\pi}_{t-1} + b_{xi} \hat{i}_{t-1} + u_{x,t}$.

C.2.4 Solving with Blanchard-Kahn

We have seen that the coefficients b_{xx}, $b_{x\pi}$, and b_{xi} are pinned down by equations (C.31) through (C.33), showing that a VAR(1) solution for the output gap exists for parts of the parameter space. However, because we are solving for three coefficients rather than one, there are no simple analytic expression for b_{xx}, $b_{x\pi}$, and b_{xi}.

We use Blanchard and Kahn (1980) to find b_{xx}, $b_{x\pi}$, and b_{xi}. This requires some simple matrix algebra, which effectively amounts to finding a rotation for b_{xx}, $b_{x\pi}$ and b_{xi} that can be easily solved.

Statement of Blanchard-Kahn

We re-state Proposition 1 of Blanchard and Kahn (1980) with an extension to the case where there are fewer eigenvalues outside the unit circle than non-predetermined variables. Let X_{t+1} be an $[n \times 1]$ vector of pre-determined variables, i.e. variables such that $E_t X_{t+1} = X_{t+1}$. Let P_{t+1} be an $[m \times 1]$ vector of non pre-determined variables, and let Z_t be a $[k \times 1]$ vector of exogenous variables. The model is given by

$$\begin{bmatrix} X_{t+1} \\ E_t P_{t+1} \end{bmatrix} = \mathcal{A} \begin{bmatrix} X_t \\ P_t \end{bmatrix} + \Gamma Z_t, \; X_{t=0} = X_0, \tag{C.37}$$

where $\mathcal{A} = [(n+m) \times (n+m)]$ and $\Gamma = [(n+m) \times k]$. The exogenous shocks Z_t are assumed to satisfy regularity conditions. While Blanchard and Kahn (1980) allow for serially correlated shocks, it is sufficient for our purposes to assume that $E_t z_{t+i} = 0 \ \forall i \geq 1$.

A solution (X_t, P_t) satisfies the model equation (C.37) for all potential realizations of the exogenous shocks. Blanchard and Kahn (1980) require that a solution satisfies the non-explosion restriction:

$$\forall t \ \exists \begin{bmatrix} \bar{X}_t \\ \bar{P}_t \end{bmatrix} \in \mathbb{R}^{n+m}, \ \sigma_t \in \mathbb{R} \text{ such that} \tag{C.38}$$

$$-(1+i)^{\sigma_t} \begin{bmatrix} \bar{X}_t \\ \bar{P}_t \end{bmatrix} \leq E_t \left(\begin{bmatrix} X_{t+i} \\ P_{t+i} \end{bmatrix} \right) \leq (1+i)^{\sigma_t} \begin{bmatrix} \bar{X}_t \\ \bar{P}_t \end{bmatrix} \ \forall i \geq 0. \tag{C.39}$$

Write the matrix $\mathcal{A}$ in the Jordan normal form:

$$\mathcal{A} = C^{-1} J C. \tag{C.40}$$

It is well-known that the Jordan normal form of a matrix is unique up to the ordering of the eigenvalues, which are listed along the diagonal in J. Further, partition J such that

$$J \ = \ \begin{bmatrix} J_1 & 0 \\ 0 & J_2 \end{bmatrix}, \tag{C.41}$$

where J_1 is $[n \times n]$ and J_2 is $[m \times m]$. The matrices C, C^{-1} and Γ are decomposed similarly:

$$C \ \equiv \ \begin{bmatrix} C_{11} & C_{12} \\ [n \times n] & [n \times m] \\ C_{21} & C_{22} \\ [m \times n] & [m \times m] \end{bmatrix}, \tag{C.42}$$

$$C^{-1} \ \equiv \ \begin{bmatrix} D_{11} & D_{12} \\ [n \times n] & [n \times m] \\ D_{21} & D_{22} \\ [m \times n] & [m \times m] \end{bmatrix}, \tag{C.43}$$

$$\Gamma \ \equiv \ \begin{bmatrix} \Gamma_1 \\ [n \times k] \\ \Gamma_2 \\ [m \times k] \end{bmatrix}. \tag{C.44}$$

Proposition 1 (Blanchard and Kahn (1980)): Assume that $\mathcal{A}$ has at least n eigenvalues within the unit circle and let (C.40) be a Jordan normal form decomposition such that all eigenvalues listed along the diagonal of J_1 are within the unit

circle. There exists a solution of the following form:

$$\begin{array}{rcll} X_t & = & X_0 & \text{for } t = 0, \\ X_t & = & B^{BK} X_{t-1} + \Sigma^{BK} Z_{t-1} & \text{for } t > 0, \end{array} \tag{C.45}$$

where the $[n \times n]$ matrix B^{BK} equals

$$B^{BK} = D_{11} J_1 D_{11}^{-1}, \tag{C.46}$$

and the $[n \times k]$ matrix Σ^{BK} equals

$$\Sigma^{BK} = \Gamma_1 - \left(D_{11} J_1 C_{12} + D_{12} J_2 C_{22}\right) C_{22}^{-1} J_2^{-1} \left(C_{21}\Gamma_1 + C_{22}\Gamma_2\right). \tag{C.47}$$

Proposition 1 of Blanchard and Kahn (1980) is originally stated for the case when the number of eigenvalues of $\mathcal{A}$ outside the unit circle is equal to the number of non-predetermined variables, m, in which case the solution is unique. When the system has more stable eigenvalues than state variables, we pick three stable eigenvalues and proceed, analogously to Uhlig (1999). A straightforward extension of the proof in Blanchard and Kahn (1980) makes clear that equations (C.45) through (C.47) still generate a solution, though this solution is no longer unique.

Proof: See section C.2.4.

Proposition 2 (Blanchard and Kahn (1980)): If the number of eigenvalues of $\mathcal{A}$ outside the unit circle is greater than the number of non-predetermined variables, m, then there exists no solution that also satisfies the non-explosion restriction.

Proof: Blanchard and Kahn (1980).

Defining the state variables

Before we can apply Blanchard-Kahn, we need to define the state vector. We define the pre-determined (i.e. known at time t) part of the state vector as:

$$X_{t+1} = \hat{Y}_t = \begin{bmatrix} x_t \\ \hat{\pi}_t \\ \hat{i}_t \end{bmatrix}. \tag{C.48}$$

The non pre-determined part of the state vector (i.e. not known at time t) is one-dimensional and equals:

$$P_{t+1} = \left[x_{t+1} + \frac{1}{\gamma}\hat{\pi}_{t+1}\right]. \tag{C.49}$$

The vector of exogenous variables (or shocks) is given by:

$$Z_t = \begin{bmatrix} v_{\pi,t} \\ v_{i,t} \\ v_t^* \end{bmatrix}. \tag{C.50}$$

We can then write the macroeconomic side of our model in matrix form:

$$\tilde{A}\begin{bmatrix} x_t \\ \hat{\pi}_t \\ \hat{i}_t \\ E_t x_{t+1} + \frac{1}{\gamma} E_t \hat{\pi}_{t+1} \end{bmatrix} = \tilde{B}\begin{bmatrix} x_{t-1} \\ \hat{\pi}_{t-1} \\ \hat{i}_{t-1} \\ x_t + \frac{1}{\gamma}\hat{\pi}_t \end{bmatrix} + \tilde{\Gamma}\begin{bmatrix} v_{\pi,t} \\ v_{i,t} \end{bmatrix}, \tag{C.51}$$

where

$$\tilde{A} = \begin{bmatrix} 1 & \frac{1}{\gamma} & 0 & 0 \\ 0 & 1 & 0 & 0 \\ 0 & 0 & 1 & 0 \\ -(\phi - \theta_1) & 0 & -\frac{1}{\gamma} & 1 \end{bmatrix} \tag{C.52}$$

$$\tilde{B} = \begin{bmatrix} 0 & 0 & 0 & 1 \\ b_{\pi x} & b_{\pi\pi} & b_{\pi i} & 0 \\ b_{ix} & b_{i\pi} & b_{ii} & 0 \\ -\theta_2 & 0 & 0 & 0 \end{bmatrix}, \tag{C.53}$$

$$\tilde{\Gamma} = \begin{bmatrix} 0 & 0 & 0 \\ 1 & 0 & 0 \\ 0 & 1 & 0 \\ 0 & 0 & 0 \end{bmatrix}. \tag{C.54}$$

The first row of (C.51) is simply the definition of the non pre-determined state variable. The second and third rows of (C.51) follow from equations (C.20) and (C.21). The third row is a simple re-arrangement of the loglinear Euler equation (C.23).

The matrix $\tilde{A}$ is invertible with

$$\tilde{A}^{-1} = \begin{bmatrix} 1 & -\frac{1}{\gamma} & 0 & 0 \\ 0 & 1 & 0 & 0 \\ 0 & 0 & 1 & 0 \\ \phi - \theta_1 & -\frac{\phi - \theta_1}{\gamma} & \frac{1}{\gamma} & 1 \end{bmatrix}, \tag{C.55}$$

so we can re-write (C.51) in the Blanchard-Kahn form:

$$\begin{bmatrix} x_t \\ \hat{\pi}_t \\ \hat{i}_t \\ E_t x_{t+1} + \frac{1}{\gamma} E_t \hat{\pi}_{t+1} \end{bmatrix} = \mathcal{A}\begin{bmatrix} x_{t-1} \\ \hat{\pi}_{t-1} \\ \hat{i}_{t-1} \\ x_t + \frac{1}{\gamma}\hat{\pi}_t \end{bmatrix} + \Gamma\begin{bmatrix} v_{\pi,t} \\ v_{i,t} \end{bmatrix}. \tag{C.56}$$

The matrices $\mathcal{A}$ and Γ are given by:

$$\mathcal{A} = \tilde{A}^{-1}\tilde{B}, \tag{C.57}$$

$$\Gamma = \tilde{A}^{-1}\tilde{\Gamma}. \tag{C.58}$$

Solving for B and Σ

From now on assume that we are in a portion of the parameter space such that $\mathcal{A}$ has three or more eigenvalues within the unit circle, so there exists a non-explosive solution. Let $\mathcal{A} = C^{-1}JC$ be a Jordan normal form decomposition, such that all eigenvalues along the diagonal of the upper-left 3×3 submatrix of J (denoted J_1) are within the unit circle. Let the matrix $D = C^{-1}$ be defined as before and let D_{11} denote the upper-left 3×3 submatrix of D. By Proposition 1 of Blanchard and Kahn (1980) there exists a $[3 \times 3]$ matrix Σ^{BK} such that the model (C.56) is solved by:

$$\underbrace{\begin{bmatrix} x_t \\ \hat{\pi}_t \\ \hat{i}_t \end{bmatrix}}_{X_{t+1}} = B^{BK} \underbrace{\begin{bmatrix} x_{t-1} \\ \hat{\pi}_{t-1} \\ \hat{i}_{t-1} \end{bmatrix}}_{X_t} + \Sigma^{BK} \underbrace{\begin{bmatrix} v_{\pi,t} \\ v_{i,t} \end{bmatrix}}_{Z_t}, \tag{C.59}$$

with

$$B^{BK} = D_{11} J_1 D_{11}^{-1}. \tag{C.60}$$

Moreover, the solution (C.59) is non-explosive.

Proposition 1 of Blanchard and Kahn (1980) provides an explicit expression for Σ^{BK}. However, in our model it is more convenient to rely on the analytic expression for the output gap shock (C.34) to derive an analytic expression for Σ^{BK}.

It is immediate that $b_{xx}^{BK}, b_{x\pi}^{BK}, b_{xi}^{BK}$, defined as the first row of the matrix $B^{BK} = D_{11} J_1 D_{11}^{-1}$, solve the coupled quadratic equations (C.31) through (C.33). By Blanchard and Kahn (1980), the dynamics (C.59) satisfy the model matrix equation (C.51), which in turn is equivalent to the full model equations (C.20), (C.21), and (C.23). Because of this equivalence, the second and third rows of B^{BK} must simply list the coefficients $b_{\pi x}, b_{\pi\pi}, b_{\pi i}$ and $b_{ix}, b_{i\pi}, b_{ix}$

$$B^{BK} = \begin{bmatrix} b_{xx}^{BK} & b_{x\pi}^{BK} & b_{xi}^{BK} \\ b_{\pi x} & b_{\pi\pi} & b_{\pi i} \\ b_{ix} & b_{i\pi} & b_{ix} \end{bmatrix}, \tag{C.61}$$

and Σ^{BK} takes the form:

$$\Sigma^{BK} = \begin{bmatrix} \sigma_{x\pi}^{BK} & \sigma_{xi}^{BK} & \sigma_{x*}^{BK} \\ 1 & 0 & 0 \\ 0 & 1 & 0 \end{bmatrix}. \tag{C.62}$$

We have already seen that the last row of (C.51) is equivalent to the loglinear Euler equation (C.23). Because the Blanchard-Kahn solution is consistent with (C.56), which in turn is equivalent to (C.51), it then follows that the output gap dynamics

$$x_t = b_{xx}^{BK} x_{t-1} + b_{x\pi}^{BK} \hat{\pi}_{t-1} + b_{xi}^{BK} \hat{i}_{t-1} + \sigma_{x\pi}^{BK} v_{\pi,t} + \sigma_{xi}^{BK} v_{i,t} + \sigma_{x*}^{BK} v_t^*, \tag{C.63}$$

combined with the inflation and interest rate dynamics (C.20) and (C.21), satisfies the Euler equation. Because (C.63) has the same form as (C.26), the algebra in section C.2.2 shows that b_{xx}^{BK}, $b_{x\pi}^{BK}$ and b_{xi}^{BK} satisfy the coupled quadratic equations (C.31) through (C.33), and $\sigma_{x\pi}^{BK} v_{\pi,t} + \sigma_{xi}^{BK} v_{i,t} + \sigma_{x*}^{BK} v_t^*$ must line up with the analytical expression for the output gap shock (C.34). This gives the following analytical expression for Σ^{BK}:

$$\Sigma^{BK} = \begin{bmatrix} \frac{b_{x\pi}^{BK} + \frac{b_{\pi\pi}}{\gamma}}{\phi - \theta_1 - b_{xx}^{BK} - \frac{1}{\gamma} b_{\pi x}} & \frac{b_{xi}^{BK} + \frac{b_{\pi i} - 1}{\gamma}}{\phi - \theta_1 - b_{xx}^{BK} - \frac{1}{\gamma} b_{\pi x}} & 0 \\ 1 & 0 & 0 \\ 0 & 1 & 0 \end{bmatrix}. \tag{C.64}$$

Proof of Blanchard and Kahn (1980)

We now reproduce the proof of Blanchard and Kahn (1980) Proposition 1. We extend the proof to show the same algebra leads to a valid (though no longer unique) solution when the matrix $\mathcal{A}$ has fewer than m eigenvalues outside the unit circle.

Consider the transformation:

$$\begin{bmatrix} Y_t \\ Q_t \end{bmatrix} = C \begin{bmatrix} X_t \\ P_t \end{bmatrix}. \tag{C.65}$$

Pre-multiplying the model equation (C.37) by C and taking expectations conditional on information at time t gives:

$$\begin{bmatrix} E_t Y_{t+1} \\ E_t Q_{t+1} \end{bmatrix} = \begin{bmatrix} J_1 & 0 \\ 0 & J_2 \end{bmatrix} \begin{bmatrix} Y_t \\ Q_t \end{bmatrix} + C\Gamma Z_t. \tag{C.66}$$

Equation (C.66) consists of two subsystems. The first n lines give a system that, by construction, is stable or borderline stable:

$$E_t Y_{t+1} = J_1 Y_t + (C_{11}\Gamma_1 + C_{12}\Gamma_2) Z_t. \tag{C.67}$$

The second system is given by

$$E_t Q_{t+1} = J_2 Q_t + (C_{21}\Gamma_1 + C_{22}\Gamma_2) Z_t. \tag{C.68}$$

There exists a non-explosive solution to (C.68) given by:

$$Q_t = -J_2^{-1}(C_{21}\Gamma_1 + C_{22}\Gamma_2) Z_t. \tag{C.69}$$

If all eigenvalues of J_2 are outside the unit circle, the process (C.69) is the unique non-explosive solution for (C.68). From now on we impose the additional condition (C.69), even if J_2 has an eigenvalue within the unit circle. If we can find a solution that satisfies (C.69), the model equation (C.37), and the non-explosion restriction, then it clearly also solves the model. Imposing this condition is our only deviation from the proof in Blanchard and Kahn (1980).

The proof in Blanchard and Kahn (1980) then shows that there is a unique solution that satisfies both the model equation (C.37) and (C.69), provided that D_{11} is invertible.[2] Consider the inverse transformation:

$$\begin{bmatrix} X_t \\ P_t \end{bmatrix} = \begin{bmatrix} D_{11} & D_{12} \\ D_{21} & D_{22} \end{bmatrix} \begin{bmatrix} Y_t \\ Q_t \end{bmatrix} \tag{C.70}$$

Because Q_0 is pinned down through (C.69), Y_0 is then uniquely determined through X_0:

$$X_0 = D_{11}Y_0 + D_{12}Q_0. \tag{C.71}$$

As X_t is predetermined, the inverse transformation (C.70) imposes the relation between innovations for Y_{t+1} and Q_{t+1}:

$$Y_{t+1} - E_tY_{t+1} = -D_{11}^{-1}D_{12}\left(Q_{t+1} - E_tQ_{t+1}\right). \tag{C.72}$$

E_0Y_1 is then uniquely determined from (C.67) and Y_1 is determined from (C.72). E_1Y_2 and Y_2 are then uniquely determined from (C.67) and (C.72) etc.

Blanchard and Kahn (1980) then apply the inverse transformation (C.70) to obtain the expression for X_t in their Proposition 1. Applying the inverse transformation to (C.66):

$$\begin{bmatrix} X_{t+1} \\ E_tP_{t+1} \end{bmatrix} = C^{-1}\begin{bmatrix} E_tY_{t+1} \\ E_tQ_{t+1} \end{bmatrix}, \tag{C.73}$$

$$= \begin{bmatrix} D_{11} & D_{12} \\ D_{21} & D_{22} \end{bmatrix} \begin{bmatrix} J_1 & 0 \\ 0 & J_2 \end{bmatrix} \begin{bmatrix} Y_t \\ Q_t \end{bmatrix} + \Gamma Z_t. \tag{C.74}$$

It follows that

$$X_{t+1} = D_{11}J_1Y_t + D_{12}J_2Q_t + \Gamma_1 Z_t, \tag{C.75}$$

$$= D_{11}J_1\left(E_{t-1}Y_t + (Y_t - E_{t-1}Y_t)\right) + D_{12}J_2Q_t + \Gamma_1 Z_t \tag{C.76}$$

With $X_t = E_{t-1}X_t$ and $E_{t-1}Q_t = 0$, the inverse transformation (C.70) gives that $X_t = D_{11}E_{t-1}Y_t$, so:

$$X_{t+1} = D_{11}J_1D_{11}^{-1}X_t - D_{11}J_1D_{11}^{-1}D_{12}Q_t + D_{12}J_2Q_t + \Gamma_1 Z_t. \tag{C.77}$$

Now because C and C^{-1} are inverses, we have that $D_{11}C_{12} + D_{12}C_{22} = 0$ or $D_{11}^{-1}D_{12} = -C_{12}C_{22}^{-1}$, so this can be re-written as:

$$X_{t+1} = D_{11}J_1D_{11}^{-1}X_t + D_{11}J_1C_{12}C_{22}^{-1}Q_t + D_{12}J_2Q_t + \Gamma_1 Z_t. \tag{C.78}$$

Substituting in for Q_t from (C.69) gives:

$$X_{t+1} = D_{11}J_1D_{11}^{-1}X_t + \Gamma_1 Z_t - \left(D_{11}J_1C_{12} + D_{12}J_2C_{22}\right)C_{22}^{-1}J_2^{-1}\left(C_{21}\Gamma_1 + C_{22}\Gamma_2\right)Z_t. \tag{C.79}$$

This completes the proof.

[2] When J_2 has one or more eigenvalues within the unit circle, this does not preclude the existence of other non-explosive model solutions that do not satisfy (C.69).

D Model solution

D.1 Summary: Macroeconomic dynamics

We now provide a brief summary of how to implement the macroeconomic solution. Derivations and explanations can be found in a separate section (Appendix C).

Define the matrix $\mathcal{A}$ as:

$$\mathcal{A} = \tilde{A}^{-1}\tilde{B}, \tag{D.1}$$

where

$$\tilde{A} = \begin{bmatrix} 1 & \frac{1}{\gamma} & 0 & 0 \\ 0 & 1 & 0 & 0 \\ 0 & 0 & 1 & 0 \\ -(\phi - \theta_1) & 0 & -\frac{1}{\gamma} & 1 \end{bmatrix}, \tag{D.2}$$

and

$$\tilde{B} = \begin{bmatrix} 0 & 0 & 0 & 1 \\ b_{\pi x} & b_{\pi\pi} & b_{\pi i} & 0 \\ b_{ix} & b_{i\pi} & b_{ii} & 0 \\ -\theta_2 & 0 & 0 & 0 \end{bmatrix}. \tag{D.3}$$

Write the matrix $\mathcal{A}$ in the Jordan normal form:

$$\mathcal{A} = C^{-1}JC. \tag{D.4}$$

It is well-known that the Jordan normal form of a matrix is unique up to the ordering of the eigenvalues, which are listed along the diagonal in J. Further, partition J such that

$$J = \begin{bmatrix} J_1 & 0 \\ 0 & J_2 \end{bmatrix}, \tag{D.5}$$

where J_1 is $[3 \times 3]$ and J_2 is $[1 \times 1]$. The matrices C, and C^{-1} are decomposed similarly:

$$C \equiv \begin{bmatrix} C_{11} & C_{12} \\ [3 \times 3] & [3 \times 1] \\ C_{21} & C_{22} \\ [1 \times 3] & [3 \times 1] \end{bmatrix}, \tag{D.6}$$

$$C^{-1} \equiv \begin{bmatrix} D_{11} & D_{12} \\ [3 \times 3] & [3 \times 1] \\ D_{21} & D_{22} \\ [1 \times 3] & [1 \times 1] \end{bmatrix}. \tag{D.7}$$

If $\mathcal{A}$ has two or fewer eigenvalues within the unit circle, we stop because there is no non-explosive equilibrium of the desired form. Otherwise, let $\mathcal{A} = C^{-1}JC$ be a Jordan normal form representation of $\mathcal{A}$, such that the eigenvalues listed in J_1, are all within the unit circle (i.e. their absolute values are less than l) and occur in complex conjugate pairs. If $\mathcal{A}$ has exactly three eigenvalues within the unit circle, J_1 is unique. If $\mathcal{A}$ has four eigenvalues within the unit circle, J_1 is not unique and each admittable ordering of the eigenvalues leads to a different solution.

The matrices B and Σ are then given by:

$$B = D_{11}J_1D_{11}^{-1}, \tag{D.8}$$

and

$$\Sigma = \begin{bmatrix} \frac{b_{x\pi}+\frac{b_{\pi\pi}}{\gamma}}{\phi-\theta_1-b_{xx}-\frac{1}{\gamma}b_{\pi x}} & \frac{b_{xi}^{BK}+\frac{b_{\pi i}-1}{\gamma}}{\phi-\theta_1-b_{xx}^{BK}-\frac{1}{\gamma}b_{\pi x}} & 0 \\ 1 & 0 & 0 \\ 0 & 1 & 0 \end{bmatrix}. \tag{D.9}$$

We find the matrices B and Σ for every ordering of the eigenvalues such that the eigenvalues listed in J_1 are within the unit circle and occur in complex conjugate pairs. When this yields more than one solution, we select between the solutions using the procedure described in the main paper.

D.1.1 Writing macroeconomic dynamics in terms of orthogonal shocks

In order to implement the numerical solution for asset prices and to simulate the model, it is convenient to re-write the macroeconomic dynamics in terms of a vector of orthogonal shocks. Recall that the standard deviations and correlations of the model shocks in equations (20)-(22) in the main paper are denoted by $\sigma_\pi, \sigma_i, \sigma_*$ and $\rho_{\pi i}, \rho_{\pi *}, \rho_{i*}$. We define a vector of orthogonal shocks $u_t = [u_{2t}, u_{3t}, u_t^*]'$ such that $u_t^* = v_t^*$ and u_t spans the vector of model shocks $v_t = [v_{\pi t}, v_{it}, v_t^*]'$.

We define the orthogonal shocks u_t via:

$$v_t = M_{temp}u_t, \tag{D.10}$$

where the invertible transformation matrix M_{temp} is given by:

$$M_{temp} = \begin{bmatrix} 1 & 0 & \frac{\rho_{\pi *}\sigma_\pi}{\sigma_*} \\ \frac{\sigma_i(\rho_{\pi i}-\rho_{\pi *}\rho_{i*})}{\sigma_\pi(1-\rho_{\pi *}^2)} & 1 & \frac{\sigma_i\rho_{i*}}{\sigma_*} \\ 0 & 0 & 1 \end{bmatrix} \tag{D.11}$$

We denote the variance-covariance matrix of the orthogonalized shocks u_t by Σ_u.

We can solve for it in terms of the model parameters and M_{temp}:

$$\begin{aligned} \Sigma_u &= E_t\left[u_t' u_t\right] && \text{(D.12)} \\ &= M_{temp}^{-1} \begin{bmatrix} \sigma_\pi^2 & \sigma_\pi\sigma_i\rho_{\pi i} & \sigma_\pi\sigma_*\rho_{\pi *}, \\ \sigma_i\sigma\pi\rho_{\pi i} & \sigma_i^2 & \sigma_i\sigma_*\rho_{i*} \\ \sigma_\pi\sigma_*\rho_{\pi *} & \sigma_i\sigma_*\rho_{i*} & \sigma_*^2 \end{bmatrix} M_{temp}^{-1'}. && \text{(D.13)} \end{aligned}$$

Macroeconomic equilibrium dynamics of the form

$$\hat{Y}_t = B\hat{Y}_{t-1} + \Sigma v_t, \tag{D.14}$$

are then equivalent to

$$\hat{Y}_t = B\hat{Y}_{t-1} + Qu_t, \tag{D.15}$$

where the matrices Σ and Q have the following one-to-one mapping:

$$Q = \Sigma M_{temp}. \tag{D.16}$$

D.2 Asset pricing recursion

Before deriving the asset pricing recursions, we derive some expressions that will be useful repeatedly. We use e_i to denote a row vector with 1 in position i and zeros elsewhere.

We can use the link between stochastically detrended consumption and the output gap (equation (2) in the main paper) to express consumption in terms of the current and lagged output gap:

$$c_t = g + c_{t-1} + x_t - \phi x_{t-1}. \tag{D.17}$$

It follows that log consumption growth equals:

$$c_{t+1} - c_t = g + x_{t+1} - \phi x_t. \tag{D.18}$$

We will substitute (D.18) repeatedly into the stochastic discount factor.

The matrix

$$Q_M = e_1 Q \tag{D.19}$$

denotes the loading of consumption innovations onto the vector of shocks u_t, where e_1 is a basis vector with a one in the first position and zeros everywhere else. The volatility of consumption surprises equals:

$$\sigma_c^2 = Q_M \Sigma_u Q_M'. \tag{D.20}$$

To simplify notation, we define $\hat{s}_t$ as the log deviation of surplus consumption from its steady state. The dynamics of $\hat{s}_t$ are:

$$\begin{aligned} \hat{s}_t &= s_t - \bar{s}, && \text{(D.21)} \\ \hat{s}_t &= \theta_0 \hat{s}_{t-1} + \theta_1 x_{t-1} + \theta_2 x_{t-2} + \lambda(\hat{s}_{t-1}) Q_M u_t, && \text{(D.22)} \end{aligned}$$

where with an abuse of notation we write:

$$\begin{aligned} \lambda(\hat{s}_t) &= \lambda_0 \sqrt{1 - 2\hat{s}_t} - 1, \hat{s}_t \leq s_{max} - \bar{s}, && \text{(D.23)} \\ \lambda(\hat{s}_t) &= 0, \hat{s}_t \geq s_{max} - \bar{s}. && \text{(D.24)} \end{aligned}$$

The steady-state surplus consumption sensitivity equals:

$$\lambda_0 = \frac{1}{\bar{S}}. \quad \text{(D.25)}$$

The steady state output gap is normalized to zero. The steady state real short-term interest rate at $x_t = 0$ and $s_t = \bar{s}$ is then the same as in Campbell-Cochrane:

$$\bar{r} = \gamma g - \frac{1}{2}\gamma^2 \sigma_c^2 / \bar{S}^2 - log(\beta). \quad \text{(D.26)}$$

In our calculations of asset prices, we repeatedly use the following expression for the expected growth in the log SDF:

$$\begin{aligned} E_t\left[m_{t+1}\right] &= \log(\beta) - \gamma g + \gamma \hat{s}_t + \gamma \phi x_t - \gamma \mathbb{E}_t \hat{s}_{t+1} - \gamma \mathbb{E}_t x_{t+1} && \text{(D.27)} \\ &= -r_t - \frac{\gamma}{2}(1 - \theta_0)(1 - 2\hat{s}_t), && \text{(D.28)} \end{aligned}$$

which follows from the asset pricing Euler equation for the real short rate. We often combine (D.28) with $r_t = \bar{r} + (e_3 - e_2 B) Z_t$.

D.2.1 State space

Our state space for solving for asset prices is five-dimensional: It consists of $\tilde{Z}_t$, which a scaled version of $\hat{Y}_t$, the surplus consumption ratio relative to steady-state $\hat{s}_t$, and the lagged output gap x_{t-1}. The lagged output gap x_{t-1} is not actually needed as a state variable and we have verified that our numerical solutions for asset prices do not vary with x_{t-1}. Our code includes x_{t-1} as a state variable for legacy reasons.

We next describe the definition of $\tilde{Z}_t$. To simplify the numerical implementation of the asset pricing recursions, it is convenient to define a scaled state vector. We require that shocks to the scaled state vector are independent standard normal and that the first dimension of the scaled state vector is perfectly correlated with output gap innovations. This rotation facilitates the numerical analysis, because it is easier to integrate over independent random variables. Aligning the first dimension of the

scaled state vector with output gap innovations (and hence surplus consumption innovations) helps, because it allows us to use a finer grid to integrate numerically over this crucial dimension, where asset prices are most nonlinear.

If the scaled state vector equals $\tilde{Z}_t = A\hat{Y}_t$ for some invertible matrix A, the dynamics of $\tilde{Z}_t$ are given by:

$$\begin{aligned} \tilde{Z}_t &= A\hat{Y}_t, & \text{(D.29)} \\ \tilde{Z}_{t+1} &= \underbrace{ABA^{-1}}_{\tilde{B}}\tilde{Z}_t + \underbrace{AQu_{t+1}}_{\epsilon_{t+1}}. & \text{(D.30)} \end{aligned}$$

What should be the variance-covariance matrix of ϵ_{t+1} and how does it constrain our choice of A? Note that the matrix Q has rank two, because the matrix Σ has rank two. We therefore want A such that the vector ϵ_{t+1} has two dimensions distributed as independent standard normals and the third one identically equal to zero. That is, we need A such that

$$\begin{aligned} Var_t\left(\epsilon_{t+1}\right) &= AQ\Sigma_u Q'A', & \text{(D.31)} \\ &= \begin{bmatrix} 1 & 0 & 0 \\ 0 & 1 & 0 \\ 0 & 0 & 0 \end{bmatrix}. & \text{(D.32)} \end{aligned}$$

Requiring that the first dimension of ϵ_{t+1} is perfectly correlated with output-gap surprises gives a second constraint for A:

$$e_1 A = \left(\sigma_c\right)^{-1} e_1. \quad \text{(D.33)}$$

Letting A_i denote the ith row of A ($i = 1, 2, 3$), we compute A using the following three steps.

1. We set

$$A_1 = \left(\sigma_c\right)^{-1} e_1. \quad \text{(D.34)}$$

   This ensures that condition (D.33) is satisfied.

2. We use the MATLAB function 'null' to compute the null space $null\left(A_1 Q\Sigma_u Q'\right)$. We define n_2 as the first vector in $null\left(A_1 Q\Sigma_u Q'\right)$, so by definition we know that $n_2\left(A_1 Q\Sigma_u Q'\right)' = 0$. We then define the second column of A as

$$A_2 = \frac{n_2}{\sqrt{n_2 Q\Sigma_u Q n_2'}}. \quad \text{(D.35)}$$

3. We define the vector $n_3 = null(Q')$, so by definition $n_3 Q = 0$. We then define the third row of A as

$$A_3 = n_3. \quad \text{(D.36)}$$

It is then straightforward to verify that (D.32) holds for

$$A = \begin{bmatrix} A_1 \\ A_2 \\ A_3 \end{bmatrix}. \tag{D.37}$$

D.2.2 Recursion for zero-coupon consumption claims

We now derive the recursion for zero-coupon consumption claims in terms of state variables $\tilde{Z}_t$, $\hat{s}_t$ and x_{t-1}. Let P^c_{nt}/C_t denote the price-dividend ratio of a zero-coupon claim on consumption at time $t+n$. The outline of our strategy here is that we first derive an analytic expression for the price-dividend ratio for P^c_{1t}/C_t. For $n \geq 1$ we guess and verify recursively that there exists a function $F_n(\tilde{Z}_t, \hat{s}_t, x_{t-1})$, such that

$$\frac{P^c_{nt}}{C_t} = F_n\left(\tilde{Z}_t, \hat{s}_t, x_{t-1}\right). \tag{D.38}$$

We start by deriving the analytic expression for F_1. The one-period zero coupon price-consumption ratio solves

$$\frac{P^c_{1,t}}{C_t} = \mathbb{E}_t\left[\frac{M_{t+1}C_{t+1}}{C_t}\right] \tag{D.39}$$

Using (D.17) to substitute for consumption growth, we factorize $M_{t+1}\frac{C_{t+1}}{C_t}$:

$$\begin{aligned} M_{t+1}\frac{C_{t+1}}{C_t} &= \beta \exp(-\gamma(\hat{s}_{t+1} - \hat{s}_t) - (\gamma-1)(c_{t+1} - c_t)) \\ &= \beta \exp(-\gamma(\hat{s}_{t+1} - \hat{s}_t) - (\gamma-1)(g + x_{t+1} - \phi x_t)) \end{aligned} \tag{D.40}$$

Using the notation $f_n = \log(F_n)$, (D.22) and (D.28) give:

$$\begin{aligned} f_1(\tilde{Z}_t, \hat{s}_t, x_{t-1}) &= \log(\beta) - (\gamma-1)\, g + \gamma \hat{s}_t + (\gamma-1)\phi x_t \\ &\quad -\gamma E_t \hat{s}_{t+1} - (\gamma-1)\, E_t x_{t+1} \\ &\quad +\frac{1}{2}(\gamma\lambda(\hat{s}_t) + (\gamma-1))^2\sigma_c^2, \\ &= g + e_1[B - \phi I]A^{-1}\tilde{Z}_t + \frac{1}{2}(\gamma\lambda(\hat{s}_t) + (\gamma-1))^2\sigma_c^2 \\ &\quad -\bar{r} - (e_3 - e_2 B)A^{-1}\tilde{Z}_t - \frac{\gamma}{2}(1-\theta_0)(1-2\hat{s}_t). \end{aligned} \tag{D.41}$$

Next, we solve for f_n, $n \geq 2$ iteratively. Note that:

$$\frac{P^c_{nt}}{C_t} = \mathbb{E}_t\left[\frac{M_{t+1}C_{t+1}}{C_t}\frac{P^c_{n-1,t+1}}{C_{t+1}}\right] = \mathbb{E}_t\left[\frac{M_{t+1}C_{t+1}}{C_t}F_{n-1}\left(\tilde{Z}_{t+1}, \hat{s}_{t+1}, x_t\right)\right] \tag{D.42}$$

This gives the following expression for f_n:

$$\begin{aligned} f_n(\tilde{Z}_t, \hat{s}_t, x_{t-1}) &= \log\Big[\mathbb{E}_t\Big[\exp\Big(\log(\beta) - (\gamma-1)g + \gamma\hat{s}_t + (\gamma-1)\phi x_t \\ &\quad -\gamma\hat{s}_{t+1} - (\gamma-1)\mathbb{E}_t x_{t+1} - (\gamma-1)e_1 A^{-1} e_1' \epsilon_{1,t+1} \\ &\quad + f_{n-1}(\tilde{Z}_{t+1}, \hat{s}_{t+1}, x_t)\Big)\Big]\Big]. \end{aligned} \tag{D.43}$$

Here, $\epsilon_{1,t+1}$ denotes the first dimension of the shock ϵ_{t+1}. We clarify that the expression in parentheses depends only on the first shock to the scaled state vector, $\epsilon_{1,t+1}$. Finally, we use (D.28) to re-write $f_{n,t}$ as an expectation involving $f_{n-1,t+1}$, the state variables $\tilde{Z}_t$, $\hat{s}_t$, and x_{t-1}, and $\epsilon_{1,t+1}$:

$$\begin{aligned} f_n(\tilde{Z}_t, \hat{s}_t, x_{t-1}) &= \log\Big[\mathbb{E}_t\Big[\exp\Big(g + e_1[B-\phi I]A^{-1}\tilde{Z}_t \\ &\quad -\bar{r} - (e_3 - e_2 B)A^{-1}\tilde{Z}_t - \frac{\gamma}{2}(1-\theta_0)(1-2\hat{s}_t) \\ &\quad -(\gamma(1+\lambda(\hat{s}_t)) - 1)\sigma_c \epsilon_{1,t+1} \\ &\quad + f_{n-1}(\tilde{Z}_{t+1}, \hat{s}_{t+1}, x_t)\Big)\Big]\Big]. \end{aligned} \tag{D.44}$$

D.2.3 Recursion for zero-coupon bond prices

We use $P^{\$}_{n,t}$ and $P_{n,t}$ denote the prices of nominal and real n-period zero-coupon bonds. The strategy is to develop analytic expressions for one- and two-period bond prices. We then guess and verify recursively that the prices of real and nominal zero-coupon bonds with maturity $n \geq 2$ can be written in the following form:

$$P_{n,t} = B_n(\tilde{Z}_t, \hat{s}_t, x_{t-1}), \tag{D.45}$$

$$P^{\$}_{n,t} = exp(-n\pi^*_t) B^{\$}_n(\tilde{Z}_t, \hat{s}_t, x_{t-1}), \tag{D.46}$$

where $B_n(\tilde{Z}_t, \hat{s}_t, x_{t-1})$ and $B^{\$}_n(\tilde{Z}_t, \hat{s}_t, x_{t-1})$ are functions of the state variables.

As discussed in the main paper, we assume that the short-term nominal interest rate contains no risk premium, so the one-period log nominal interest rate equals $i_t = r_t + E_t\pi_{t+1}$. The means of $\hat{i}_t$ and $\hat{\pi}_t$ are normalized to zero, but in order to derive bond prices we need to account for the average level of interest rates. We do this by writing the one-period log nominal interest rate as $i_t = \hat{i}_t + \pi^*_t + \bar{r}$ and the one-period log real interest rate as $r_t = \hat{i}_t - E_t\hat{\pi}_{t+1} + \bar{r}$. One-period bond prices then equal:

$$P^{\$}_{1,t} = \exp(-\hat{i}_t - \pi_{*t} - \bar{r}), \tag{D.47}$$

$$P_{1,t} = \exp(-\hat{i}_t + \mathbb{E}_t\hat{\pi}_{t+1} - \bar{r}). \tag{D.48}$$

We next solve for longer-term bond prices including risk premia. Substituting in

(D.47) into the bond-pricing recursion gives:

$$\begin{aligned} P^{\$}_{2,t} &= \mathbb{E}_t\left[M_{t+1}P^{\$}_{1,t+1}\exp(-\pi^*_{t+1}-\hat{\pi}_{t+1})\right] && \text{(D.49)}\\ &= \mathbb{E}_t\left[M_{t+1}\exp(-\hat{i}_{t+1}-2\pi^*_{t+1}-\hat{\pi}_{t+1}-\bar{r})\right] && \text{(D.50)}\\ &= \beta\mathbb{E}_t\left[\exp(-\gamma(\hat{s}_{t+1}-\hat{s}_t)-\gamma(g+x_{t+1}-\phi x_t)-\hat{i}_{t+1}-2\pi^*_{t+1}-\hat{\pi}_{t+1}-\bar{r}))\right]. && \text{(D.51)}\end{aligned}$$

We can now verify that the two-period nominal bond price takes the form (D.46):

$$\begin{aligned} B^{\$}_2(\tilde{Z}_t,\hat{s}_t,x_{t-1}) &= \exp\left(\log(\beta)-\gamma g+\gamma\hat{s}_t+\gamma\phi x_t\right)\\ &\quad\times\exp\left(\mathbb{E}_t\left(-\gamma\hat{s}_{t+1}-\gamma x_{t+1}-\hat{i}_{t+1}-\hat{\pi}_{t+1}-\bar{r}\right)\right)\\ &\quad\times\mathbb{E}_t\left[\exp\left(\left(-\gamma\left(\lambda(\hat{s}_t)+1\right)Q_M-\underbrace{[(e_2+e_3)Q+2e_3]}_{v_{\$}}\right)u_{t+1}\right)\right]. \end{aligned} \quad \text{(D.52)}$$

Here, we define the vector $v_{\$}$ to simplify notation. The random walk component of inflation π^*_t does not appear in (D.52), because $B^{\$}_2$ is already scaled by $exp(-2\pi^*_t)$ by definition (D.46). Taking logs, applying (D.28), and using the definition for the sensitivity function $\lambda(\hat{s}_t)$, we get:

$$\begin{aligned} b^{\$}_2 &= -e_3[I+B]A^{-1}\tilde{Z}_t+\frac{1}{2}v_{\$}\Sigma_u v_{\$}\prime\\ &\quad+\gamma\left(\lambda(\hat{s}_t)+1\right)Q_M\Sigma_u v'_{\$}-2\bar{r}. \end{aligned} \quad \text{(D.53)}$$

We similarly solve for two-period real bond prices in closed form:

$$\begin{aligned} P_{2,t} &= \exp\left(\log(\beta)-\gamma g+\gamma\hat{s}_t+\gamma\phi x_t\right)\\ &\quad\times\exp\left(\mathbb{E}_t\left(-\gamma\hat{s}_{t+1}-\gamma x_{t+1}-\hat{i}_{t+1}+\mathbb{E}_{t+1}\hat{\pi}_{t+2}-\bar{r}\right)\right)\\ &\quad\times\mathbb{E}_t\left[\exp\left((-\gamma(\lambda(\hat{s}_t)+1)Q_M-\underbrace{(e_3-e_2B)Q}_{v_r})u_{t+1}\right)\right] \end{aligned} \quad \text{(D.54)}$$

We define the vector v_r to simplify notation. Taking logs, applying (D.28), and using the definition for $\lambda(\hat{s}_t)$ gives:

$$b_2(\tilde{Z}_t,\hat{s}_t,x_{t-1}) = -(e_3-e_2B)\left[I+B\right]A^{-1}\tilde{Z}_t+\frac{1}{2}v_r\Sigma_u v'_r+\gamma\left(\lambda(\hat{s}_t)+1\right)Q_M\Sigma_u v'_r-2\bar{r}. \quad \text{(D.55)}$$

For $n \geq 3$, we use (D.28) to obtain the following recursion for real bond prices:

$$\begin{aligned} B_n(\tilde{Z}_t, \hat{s}_t, x_{t-1}) &= \mathbb{E}_t \left[\exp \left(\log(\beta) - \gamma g + \gamma \hat{s}_t \right. \right. \qquad \text{(D.56)} \\ &\quad \left. \left. -\gamma \hat{s}_{t+1} + \gamma \phi x_t - \gamma x_{t+1} + b_{n-1}(\tilde{Z}_{t+1}, \hat{s}_{t+1}, x_t) \right) \right] \\ &= \mathbb{E}_t \left[\exp \left(-\bar{r} - (e_3 - e_2 B) A^{-1} \tilde{Z}_t - \frac{\gamma}{2}(1-\theta_0)(1-2\hat{s}_t) \right. \right. \\ &\quad \left. \left. -\gamma(1+\lambda(\hat{s}_t))\sigma_c \epsilon_{1,t+1} + b_{n-1}(\tilde{Z}_{t+1}, \hat{s}_{t+1}, x_t) \right) \right]. \qquad \text{(D.57)} \end{aligned}$$

The recursion for nominal bond prices with $n \geq 3$ is similar. It is complicated by the fact that we need to integrate over shocks to the inflation target:

$$\begin{aligned} B_n^{\$}(\tilde{Z}_t, \hat{s}_t, x_{t-1}) &= \mathbb{E}_t \left[\exp \left(\log(\beta) - \gamma g + \gamma \hat{s}_t + \gamma \phi x_t \right. \right. \qquad \text{(D.58)} \\ &\quad \left. \left. -\gamma \hat{s}_{t+1} - \gamma x_{t+1} - \hat{\pi}_{t+1} - n u^*_{t+1} + b^{\$}_{n-1}(\tilde{Z}_{t+1}, \hat{s}_{t+1}, x_t) \right) \right]. \end{aligned}$$

To reduce the number of dimensions along which we need to integrate numerically, we split u^*_{t+1} into a component that is spanned by ϵ_{t+1} plus an orthogonal shock. This is useful because we can then use analytic expressions to integrate over the orthogonal component. We use the standard expression for conditional distributions of multivariate normal random variables. The distribution of u^*_{t+1} conditional on ϵ_{t+1} is normal with:

$$u^*_{t+1} \,|\epsilon_{t+1} \sim N \left(\underbrace{(AQ\Sigma_u e_3')'}_{vec_*} \epsilon_{t+1}, \underbrace{(\sigma^*)^2 - (AQ\Sigma_u e_3')'(AQ\Sigma_u e_3')}_{(\sigma^\perp)^2} \right). \qquad \text{(D.59)}$$

We then write u^*_t as the sum of two independent shocks:

$$u^*_{t+1} = vec^* \epsilon_{t+1} + \epsilon^\perp_{t+1}, \qquad \text{(D.60)}$$

where $\epsilon^\perp_{t+1}$ is defined as

$$\epsilon^\perp_{t+1} := u^*_{t+1} - vec^* \epsilon_{t+1} \qquad \text{(D.61)}$$

We integrate analytically over $\epsilon^\perp_{t+1}$ and substitute in (D.28):

$$\begin{aligned} B_n^{\$}(\tilde{Z}_t, \hat{s}_t, x_{t-1}) &= \mathbb{E}_t \left[\exp \left(\log(\beta) - \gamma g + \gamma \hat{s}_t + \gamma \phi x_t - \gamma \hat{s}_{t+1} - \gamma x_{t+1} \right. \right. \\ &\quad \left. \left. -\hat{\pi}_{t+1} - n vec^* \epsilon_{t+1} + \frac{n^2}{2}(\sigma^\perp)^2 + b^{\$}_{n-1}(\tilde{Z}_{t+1}, \hat{s}_{t+1}, B^{\$} x_t) \right) \right], \\ &= \mathbb{E}_t \left[\exp \left(-\bar{r} - e_3 A^{-1} \tilde{Z}_t - \frac{\gamma}{2}(1-\theta_0)(1-2\hat{s}_t) \right. \right. \\ &\quad -(\gamma(1+\lambda(\hat{s}_t))\sigma_c + \underbrace{e_2 A^{-1} e_1'}_{vpi_1} + n vec^* e_1') \epsilon_{1,t+1} \\ &\quad - \left(\underbrace{e_2 A^{-1} e_2'}_{vpi_2} + n vec^* e_2' \right) \epsilon_{2,t+1} \\ &\quad \left. \left. + \frac{n^2}{2}(\sigma^\perp)^2 + b^{\$}_{n-1}(\tilde{Z}_{t+1}, \hat{s}_{t+1}, x_t) \right) \right]. \qquad \text{(D.62)} \end{aligned}$$

We define the vectors vpi_1 and vpi_2 as given above to avoid computing them repeatedly in our numerical algorithm.

D.2.4 Assessing the approximation error for the one-period nominal rate

Throughout the paper, we use the approximation

$$i_t = r_t + E_t \pi_{t+1}. \tag{D.63}$$

This approximation is useful, because it leads to log-linear macroeconomic dynamics in the output gap, inflation, and the nominal interest rate. In order to undestand the significance of the error in this approximation, we now derive the exact one-period nominal bond yield while taking the dynamics for real consumption and the real interest rate as given. The exact one-period nominal bond price equals:

$$\begin{aligned} P_{1,t}^{\$,exact} &= \exp\left(\log(\beta) - \gamma g + \gamma \hat{s}_t + \gamma \phi x_t\right) \\ &\quad \times \exp\left(\mathbb{E}_t\left(-\gamma \hat{s}_{t+1} - \gamma x_{t+1} - \hat{\pi}_{t+1} - \pi_{t+1}^*\right)\right) \\ &\quad \times \mathbb{E}_t\left[\exp\left(\left(-\gamma\left(\lambda(\hat{s}_t)+1\right) Q_M - \left[e_2 Q + e_3\right]\right) u_{t+1}\right)\right]. \end{aligned} \tag{D.64}$$

We now substitute in (D.28), and take logs to get:

$$\begin{aligned} \log\left(P_{1,t}^{\$,exact}\right) &= -r_t - E_t \pi_{t+1} \\ &\quad + \frac{1}{2}\left(e_2 Q + e_3\right) \Sigma_u \left(e_2 Q + e_3\right)' + \gamma\left(\lambda(\hat{s}_t)+1\right) Q_M \Sigma_u \left(e_2 Q + e_3\right)'. \end{aligned} \tag{D.65}$$

We decompose the one-period nominal bond yield into the approximate nominal yield, i_t, and approximation error:

$$\begin{aligned} y_{1,t}^{\$,exact} &= \underbrace{r_t + E_t \pi_{t+1}}_{i_t} \\ &\quad \underbrace{-\frac{1}{2}\left(e_2 Q + e_3\right) \Sigma_u \left(e_2 Q + e_3\right)' - \gamma\left(\lambda(\hat{s}_t)+1\right) Q_M \Sigma_u \left(e_2 Q + e_3\right)'}_{\text{Approximation Error}} \end{aligned} \tag{D.66}$$

At our point estimates, we find that the simulated approximation error has a standard deviation of 4bps.

D.2.5 Computing returns

The log return on the consumption claim equals:

$$r_{t+1}^c = \log\left(\frac{P_{t+1}^c + C_{t+1}}{P_t^c}\right), \tag{D.67}$$

$$= \Delta c_{t+1} + \log\left(\frac{1 + \frac{P_{t+1}^c}{C_{t+1}}}{\frac{P_t^c}{C_t}}\right). \tag{D.68}$$

Real and nominal log bond yields equal:

$$y_{n,t} = -\frac{1}{n} b_{n,t}, \tag{D.69}$$

$$y_{n,t}^{\$} = -\frac{1}{n} b_{n,t}^{\$} + \pi_t^*. \tag{D.70}$$

Real log bond returns equal:

$$r_{n,t+1} = b_{n-1,t+1} - b_{n,t}. \tag{D.71}$$

Nominal log bond returns equal:

$$r_{n,t+1}^{\$} = b_{n-1,t+1}^{\$} - b_{n,t}^{\$} - (n-1)\pi_{t+1}^* + n\pi_t^*. \tag{D.72}$$

Real and nominal bond log excess returns then equal:

$$xr_{n,t+1} = r_{n,t+1} - r_t, \tag{D.73}$$

$$xr_{n,t+1}^{\$} = r_{n,t+1}^{\$} - i_t. \tag{D.74}$$

D.2.6 Levered stock prices and returns

We note that the price of the levered equity claim is δP_t^c, so the price-dividend ratio equals:

$$\frac{P_t^\delta}{D_t^\delta} = \delta \frac{C_t}{D_t^\delta} \frac{P_t^c}{C_t}. \tag{D.75}$$

Using the expression

$$D_{t+1}^\delta = P_{t+1}^c + C_{t+1} - (1-\delta) P_t^c \exp(r_t) - \delta P_t^c, \tag{D.76}$$

and

$$P_t^\delta = \delta P_t^c \tag{D.77}$$

gives the gross return on levered stocks:

$$\begin{aligned}
\left(1+R^{\delta}_{t+1}\right) &= \frac{D^{\delta}_{t+1}+P^{\delta}_{t+1}}{P^{\delta}_{t}}, && \text{(D.78)}\\
&= \frac{1}{\delta}\frac{P^{c}_{t+1}+C_{t+1}-(1-\delta)P^{c}_{t}exp(r_t)}{P^{c}_{t}}, && \text{(D.79)}\\
&= \frac{1}{\delta}\left(1+R^{c}_{t+1}\right)-\frac{1-\delta}{\delta}exp\left(r_t\right). && \text{(D.80)}
\end{aligned}$$

Log stock excess returns then equal:

$$xr^{\delta}_{t+1} = r^{\delta}_{t+1}-r_t. \quad \text{(D.81)}$$

To mimic firms' dividend smoothing in the data, we report simulated moments for the price of equities dividend by dividends smoothed over the past 64 quarters:

$$P^{\delta}_{t}/\left(\frac{1}{64}(D^{\delta}_{t}+D^{\delta}_{t-1}+...+D^{\delta}_{t-63})\right). \quad \text{(D.82)}$$

D.3 Details: Risk-premium decomposition

For the risk-premium decomposition in Table 5 in the main paper, we use the following steps. We first compute risk-neutral valuations and returns. We then decompose risk-neutral returns further into news about the real interest rate and news about cash flows using the Campbell and Ammer (1993) loglinear expressions. We then define returns due to risk premia as log asset excess returns minus risk-neutral returns. We use the superscript ^{rn} for risk-neutral, superscript ^{cf} for cash flow, and ^{rp} for risk premium.

Risk-neutral valuations are expected cash flows discounted with the risk-neutral discount factor, that is consistent with equilibrium dynamics for the real interest rate:

$$\begin{aligned}
M^{rn}_{t+1} &= exp(-r_t) && \text{(D.83)}\\
&= \exp(-\hat{i}_t+\mathbb{E}_t\hat{\pi}_{t+1}-\bar{r}). && \text{(D.84)}
\end{aligned}$$

D.3.1 Risk-neutral zero-coupon bond prices

We use analogous recursions to solve for risk-neutral bond prices. One-period risk-neutral bond prices are given exactly as before:

$$\begin{aligned}
P^{\$,rn}_{1,t} &= \exp(-\hat{i}_t-\pi^{*}_{t}-\bar{r}), && \text{(D.85)}\\
P^{rn}_{1,t} &= \exp(-\hat{i}_t+\mathbb{E}_t\hat{\pi}_{t+1}-\bar{r}). && \text{(D.86)}
\end{aligned}$$

For $n > 1$, we guess and verify that the prices of real and nominal risk-neutral zero-coupon bonds with maturity n can be written in the following form

$$\begin{aligned} P_{n,t}^{rn} &= B_n^{rn}(\tilde{Z}_t, \hat{s}_t, x_{t-1}), && \text{(D.87)} \\ P_{n,t}^{\$,rn} &= exp(-n\pi_t^*) B_n^{\$,rn}(\tilde{Z}_t, \hat{s}_t, x_{t-1}). && \text{(D.88)} \end{aligned}$$

for some functions $B_n^{rn}(\tilde{Z}_t, \hat{s}_t, x_{t-1})$ and $B_n^{\$,rn}(\tilde{Z}_t, \hat{s}_t, x_{t-1})$.

We derive the two-period risk-neutral nominal bond price analytically:

$$\begin{aligned} P_{2,t}^{\$,rn} &= exp(-r_t)\mathbb{E}_t\left[P_{1,t+1}^{\$,rn} \exp(-\pi_{t+1}^* - \hat{\pi}_{t+1})\right] && \text{(D.89)} \\ &= exp(-r_t)\mathbb{E}_t\left[\exp(-\hat{i}_{t+1} - 2\pi_{t+1}^* - \hat{\pi}_{t+1} - \bar{r})\right]. && \text{(D.90)} \end{aligned}$$

We can hence verify that the two-period risk-neutral nominal bond price takes the form (D.46) with:

$$\begin{aligned} B_2^{\$,rn}(\tilde{Z}_t, \hat{s}_t, x_{t-1}) &= \exp\left(-\hat{i}_t + \mathbb{E}_t\hat{\pi}_{t+1} - \bar{r}\right) \exp\left(\mathbb{E}_t\left(-\hat{i}_{t+1} - \hat{\pi}_{t+1} - \bar{r}\right)\right) \\ &\quad \times \mathbb{E}_t\left[\exp\left(\left(-\underbrace{[(e_2+e_3)Q + 2e_3]}_{v_\$}\right) u_{t+1}\right)\right]. \end{aligned} \tag{D.91}$$

Here, the vector $v_\$$ is identical to the case with risk aversion. Taking logs, we get:

$$b_2^{\$,rn} = -e_3\left[I + B\right]A^{-1}\tilde{Z}_t + \frac{1}{2}v_\$\Sigma_u v_\$\prime - 2\bar{r} \tag{D.92}$$

Comparing expressions (D.92) and (D.53) shows that they agree when $\gamma = 0$. We similarly solve for 2-period real bond prices in closed form:

$$\begin{aligned} P_{2,t}^{rn} &= \exp\left(-\hat{i}_t + \mathbb{E}_t\hat{\pi}_{t+1} - \bar{r}\right) \times \exp\left(\mathbb{E}_t\left(-\hat{i}_{t+1} + \mathbb{E}_{t+1}\hat{\pi}_{t+2} - \bar{r}\right)\right) \\ &\quad \times \mathbb{E}_t\left[\exp\left(-\underbrace{(e_3 - e_2B)Q}_{v_r} u_{t+1}\right)\right]. \end{aligned} \tag{D.93}$$

The vector v_r is again identical to the case with risk aversion. Taking logs gives:

$$b_2^{rn}(\tilde{Z}_t, \hat{s}_t, x_{t-1}) = -(e_3 - e_2B)\left[I + B\right]A^{-1}\tilde{Z}_t + \frac{1}{2}v_r\Sigma_u v_r' - 2\bar{r}. \tag{D.94}$$

We note that the risk-neutral bond prices (D.94) and bond prices with risk aversion (D.55) are identical when the utility curvature parameter γ equals zero.

For $n \geq 3$ the n-period risk neutral real bond price B_n^{rn} satisfies the recursion:

$$B_n^{rn}(\tilde{Z}_t, \hat{s}_t, x_{t-1}) = \mathbb{E}_t\left[\exp\left(-\bar{r} - (e_3 - e_2B)A^{-1}\tilde{Z}_t + b_{n-1}(\tilde{Z}_{t+1}, \hat{s}_{t+1}, x_t)\right)\right] \tag{D.95}$$

We obtain a similar recursion for risk-neutral nominal bond prices:

$$B_n^{\$,rn}(\tilde{Z}_t, \hat{s}_t, x_{t-1}) = \mathbb{E}_t\left[\exp\left(-\hat{i}_t + \mathbb{E}_t\hat{\pi}_{t+1} - \bar{r} - \hat{\pi}_{t+1} - nu_{t+1}^* + b_{n-1}^{\$}(\tilde{Z}_{t+1}, \hat{s}_{t+1}, x_t)\right)\right].$$

We again use the decomposition $u_{t+1}^* = vec^*\epsilon_{t+1} + \epsilon_{t+1}^{\perp}$ from Section D.2.3 to reduce the dimensionality of the numerical integration:

$$\begin{aligned} B_n^{\$,rn}(\tilde{Z}_t, \hat{s}_t, x_{t-1}) &= \mathbb{E}_t\left[\exp\left(-\hat{i}_t + \mathbb{E}_t\hat{\pi}_{t+1} - \bar{r} - \hat{\pi}_{t+1} - n\cdot vec^*\epsilon_{t+1} + \frac{n^2}{2}(\sigma^{\perp})^2\right.\right. \qquad \text{(D.96)}\\ &\quad \left.\left. + b_{n-1}^{\$}(\tilde{Z}_{t+1}, \hat{s}_{t+1}, B^{\$}x_t)\right)\right], \\ &= \mathbb{E}_t\left[\exp\left(-\bar{r} - e_3A^{-1}\tilde{Z}_t - (\underbrace{e_2A^{-1}e_1'}_{vpi_1} + n\cdot vec^*e_1')\epsilon_{1,t+1}\right.\right. \\ &\quad \left.\left. - \left(\underbrace{e_2A^{-1}e_2'}_{vpi_2} + n\cdot vec^*e_2'\right)\epsilon_{2,t+1} + \frac{n^2}{2}(\sigma^{\perp})^2 + b_{n-1}^{\$}(\tilde{Z}_{t+1}, \hat{s}_{t+1}, x_t)\right)\right]. \qquad \text{(D.97)} \end{aligned}$$

D.3.2 Risk-neutral zero-coupon consumption claims

Next, we derive recursive solutions for the risk-neutral prices of zero-coupon consumption claims. Let $P_{nt}^{c,rn}/C_t$ denote the risk-neutral price-dividend ratio of a zero-coupon claim on consumption at time $t+n$. The risk-neutral price-consumption ratio of a claim to the entire stream of future consumption equals:

$$\frac{P_t^{c,rn}}{C_t} = \sum_{n=1}^{\infty}\frac{P_{nt}^{c,rn}}{C_t}. \qquad \text{(D.98)}$$

For $n \geq 1$, we guess and verify there exists a function $F_n^{rn}(\tilde{Z}_t, \hat{s}_t, x_{t-1})$, such that

$$\frac{P_{nt}^{c,rn}}{C_t} = F_n^{rn}\left(\tilde{Z}_t, \hat{s}_t, x_{t-1}\right). \qquad \text{(D.99)}$$

We start by deriving the analytic expression for F_1^{rn}. The one-period risk-neutral zero-coupon price-consumption ratio solves

$$\frac{P_{1,t}^{c,rn}}{C_t} = exp\left(-\hat{i}_t + \mathbb{E}_t\hat{\pi}_{t+1} - \bar{r}\right)\mathbb{E}_t\left[\frac{C_{t+1}}{C_t}\right] \qquad \text{(D.100)}$$

Using (D.17) to substitute for consumption growth, we can derive the following analytic expression for f_1^{rn}:

$$\begin{aligned} f_1^{rn}(\tilde{Z}_t, \hat{s}_t, x_{t-1}) &= -\hat{i}_t + \mathbb{E}_t\hat{\pi}_{t+1} - \bar{r} + g - \phi x_t + E_t x_{t+1} + \frac{1}{2}\sigma_c^2, \\ &= -\left(e_3 - e_2B\right)A^{-1}\tilde{Z}_t - \bar{r} + g + e_1[B - \phi I]A^{-1}\tilde{Z}_t + \frac{1}{2}\sigma_c^2. \end{aligned} \qquad \text{(D.101)}$$

Next, we solve for f_n, $n \geq 2$ iteratively:

$$\frac{P_{nt}^{c,rn}}{C_t} = exp\left(-\hat{i}_t + \mathbb{E}_t\hat{\pi}_{t+1} - \bar{r}\right)\mathbb{E}_t\left[\frac{C_{t+1}}{C_t}F_{n-1}^{rn}\left(\tilde{Z}_{t+1}, \hat{s}_{t+1}, x_t\right)\right] \quad \text{(D.102)}$$

This gives the following expression for f_n^{rn}:

$$f_n^{rn}(\tilde{Z}_t, \hat{s}_t, x_{t-1}) = \log\left[\mathbb{E}_t\left[\exp\left(-\hat{i}_t + \mathbb{E}_t\hat{\pi}_{t+1} - \bar{r} + g - \phi x_t + \mathbb{E}_t x_{t+1} + \sigma_c\epsilon_{1,t+1} + f_{n-1}^{rn}(\tilde{Z}_{t+1}, \hat{s}_{t+1}, x_t)\right)\right]\right]. \quad \text{(D.103)}$$

Finally, we re-write $f_{n,t}^{rn}$ as an expectation involving $f_{n-1,t+1}^{rn}$, the state variables $\tilde{Z}_t$, and period $t+1$ shocks:

$$f_n^{rn}(\tilde{Z}_t, \hat{s}_t, x_{t-1}) = \log\left[\mathbb{E}_t\left[\exp\left(g + e_1[B - \phi I]A^{-1}\tilde{Z}_t - \bar{r} - (e_3 - e_2 B)A^{-1}\tilde{Z}_t + \sigma_c\epsilon_{1,t+1} + f_{n-1}^{rn}(\tilde{Z}_{t+1}, \hat{s}_{t+1}, x_t)\right)\right]\right]. \quad \text{(D.104)}$$

D.3.3 Risk-neutral returns

We plug risk-neutral price-consumption ratios and bond prices into equations (D.68) through (D.74). This gives risk-neutral returns on the consumption claim, risk-neutral log excess bond returns, and risk-neutral bond yields. We then substitute risk-neutral returns on the consumption claim into (D.80)-(D.81) to obtain risk-neutral log excess stock returns.

D.3.4 Cash-flow news, real-rate news, and risk-premium excess returns

We decompose risk-neutral returns further into cash-flow news and real-rate news. We use the approximate log-linear decomposition of Campbell and Shiller (1988):

$$\begin{aligned} xr_{t+1}^{\delta,rn} &= r_{t+1}^{\delta,rn} - r_t, && \text{(D.105)} \\ &= r_{t+1}^{\delta,rn} - E_t r_{t+1}^{\delta,rn} && \text{(D.106)} \\ &= \underbrace{(E_{t+1} - E_t)\sum_{j=0}^{\infty}\rho^j \Delta d_{t+1+j}}_{\text{Cash Flow News}} - \underbrace{(E_{t+1} - E_t)\sum_{j=1}^{\infty}\rho^j r_{t+j}}_{\text{Real Rate News}}. && \text{(D.107)} \end{aligned}$$

The first equality follows, because the risk neutral SDF ensures that expected risk neutral returns are equal to the real risk-free rate r_t. Here, ρ is the log-linearization constant corresponding to the risk-neutral price-dividend ratio

$$\rho = \frac{1}{1 + exp\left(mean(pd^{\delta,rn})\right)}, \quad \text{(D.108)}$$

and $mean(pd^{rn})$ denotes the average risk-neutral log price-dividend ratio, which in practice we obtain from 2 model simulations of length 10000.

We use the following analytic expression for the equity excess returns due to real-rate news:

$$\begin{aligned} xr_{t+1}^{\delta,rr} &= -\left(E_{t+1}-E_t\right)\sum_{j=1}^{\infty}\rho^j r_{t+j} && \text{(D.109)}\\ &= -\rho\left(e_3-e_2B\right)\left(I-\rho B\right)^{-1}Qu_{t+1}. && \text{(D.110)}\end{aligned}$$

We obtain cash-flow news as risk-neutral excess returns minus returns due to real-rate news:

$$xr_{t+1}^{\delta,cf} = xr_{t+1}^{\delta,rn}+\rho\left(e_3-e_2B\right)\left(I-\rho B\right)^{-1}Qu_{t+1} \quad \text{(D.111)}$$

The risk-premium component of equity excess returns equals log excess stock returns minus risk-neutral excess returns:

$$xr_{t+1}^{\delta,rp} = xr_{t+1}^{\delta}-xr_{t+1}^{\delta,rn}. \quad \text{(D.112)}$$

We similarly decompose bond returns into cash-flow news, real-rate news, and risk-premium excess returns, using the log-linear exact expression from Campbell and Ammer (1993):

$$\begin{aligned} xr_{n,t+1}^{\$,rn} &= r_{t+1}^{\$,rn}-i_t, && \text{(D.113)}\\ &= r_{n,t+1}^{\$,rn}-E_t r_{n,t+1}^{\$,rn}, && \text{(D.114)}\\ &= \left(E_{t+1}-E_t\right)\left\{-\sum_{i=1}^{n-1}\pi_{t+1+i}-\sum_{i=1}^{n-1}r_{t+1+i}\right\}. && \text{(D.115)}\end{aligned}$$

The real-rate news component of nominal bond log excess returns is simply the risk-neutral log excess return on a real n-period bond

$$\begin{aligned} xr_{n,t+1}^{\$,rr} &= \left(E_{t+1}-E_t\right)\sum_{i=1}^{n-1}r_{t+1+i}, && \text{(D.116)}\\ &= xr_{t+1}^{rn}. && \text{(D.117)}\end{aligned}$$

With this, we compute the cash-flow news component of nominal bond returns:

$$xr^{\$,cf} = xr_{t+1}^{\$,rn}-xr_{t+1}^{rn}. \quad \text{(D.118)}$$

The risk-premium component of log excess nominal bond returns is defined as the log excess return minus the risk-neutral log excess return:

$$xr_{t+1}^{\$,rp} = xr_{t+1}^{\$}-xr_{t+1}^{\$,rn}. \quad \text{(D.119)}$$

E Details: Numerical algorithm

Since our preferences nest Campbell-Cochrane, a minimum requirement for any numerical solution method is that it must be accurate for the original Campbell-Cochrane model and calibration. We evaluate asset prices by iterating on a grid for the state vector following Wachter (2005). Other numerical methodologies are faster, but their cost is that they cannot replicate the economic properties of Wachter (2005)'s numerical solution for Campbell-Cochrane. In unreported results, we verified that analytic linear approximations to the sensitivity function λ (e.g. Lopez, López-Salido, and Vazquez-Grande 2015), numerical higher-order perturbation methods using Dynare (Rudebusch and Swanson 2008), and global projection methods give solutions for Campbell-Cochrane that are economically very different from Wachter (2005)'s numerical solution.

Other approaches in the literature are also not appropriate for our problem. While Chen (2017) solves a model with habit and production using global projection and perturbation methods, his model features a linear sensitivity function and heteroskedastic consumption. By contrast, we have homoskedastic consumption and a highly nonlinear sensitivity function. Similarly, affine term structure models, such as Dai and Singleton (2000), generate affine relations between risk premia and state variables by assuming analytically convenient functional forms for the pricing kernel. In contrast to models that assume more convenient pricing kernels, our preferences are consistent with the standard log-linear New Keynesian consumption Euler equation and generate conditionally homoskedastic macroeconomic dynamics.

While iterating on a grid is significantly slower than perturbation or global projection methods, it is not prohibitively so. Our MATLAB algorithm for solving the asset pricing recursions (described in Section E.1) takes 80 seconds to run on a Lenovo X270 laptop with an i7-7600 CPU. Simulating the model (described in Section E.2) takes 11 seconds. The risk-neutral asset pricing recursions and simulating the risk-neutral stock returns take an additional 80 seconds and 11 seconds. MATLAB is not a particularly efficient programming language, so it is plausible that further speed ups are possible by using a lower-level programming language, such as FORTRAN or C.

E.1 Implementing the asset pricing recursions

We implement the recursions in Sections D.2.2 and D.2.3 numerically through value function iteration on a grid. We solve for the functions f_n, b_n, and $b_n^{\$}$ using value function iteration along a five-dimensional state vector. We use a five-dimensional grid, with the first three dimensions corresponding to $\tilde{Z}_t$, the fourth dimension corresponding to $\hat{s}_t$, and the fifth dimension corresponding to x_{t-1}.

E.1.1 Grid

In this section, we use $\tilde{Z}, \hat{s}, x$ to denote the corresponding time-t variables. We use superscripts $^-$ to denote variables in the previous period and $^+$ to denote variables in the next period. We solve numerically for f_n, b_n, and $b_n^\$$ as functions of the vector of state variables $\left[\tilde{Z}, \hat{s}, x^-\right]$.

Our grid is densest along the $\hat{s}$ dimension to capture important non-linearities of asset prices with respect to the surplus consumption ratio. Following Wachter (2005), we choose a grid for the surplus consumption ratio that consists of an upper segment and a lower segment and covers a wide range of values for s_t. Let $S_{grid,1}$ denote a vector of 20 equally spaced points between 0 and S_{max} with S_{max} included and $s_{grid,2}$ a vector of 30 equally spaced points between $min\left(\log\left(S_{grid,1}\right)\right)$, and -50. The grid for $\hat{s}_t = s_t - \bar{s}$ then consists of the concatenation of $s_{grid,2} - \bar{s}$ and $\log\left(S_{grid,1}\right) - \bar{s}$.

We find that bond and stock prices are close to loglinear in $\tilde{Z}$ and $\hat{x}^-$, so coarser grids are sufficient along those dimensions of the state vector. In fact, the analytic expressions for f_1, b_2, and $b_2^\$$ show that one-period zero-coupon consumption claims and two-period bond prices are exactly log-linear in $\tilde{Z}$ and x^-. Numerical results indicate that this property translates to longer-period claims and f_n, b_n, and $b_n^\$$ are still approximately linear in $\tilde{Z}$ and x^- for general n. To speed up the value function iteration, we therefore use two grid points for each dimension of $\tilde{Z}$ and for x^-.

For $\tilde{Z}$, we use an equal-spaced three-dimensional grid. Let N denote the number of grid points along each dimension and m the width of the grid as a multiple of the unconditional standard deviation of $\tilde{Z}$. For each dimension of $\tilde{Z}$, we choose a grid of N equal-spaced points with the lowest point equal to $-m \times std(\tilde{Z})$ and the highest point equal to $m \times std(\tilde{Z})$. Here, the unconditional variance-covariance matrix of $\tilde{Z}$ is determined implicitly by the equation:

$$std(\tilde{Z}) \;=\; \sqrt{\tilde{B} Var\left(\tilde{Z}\right) \tilde{B}' + diag(1,1,0)}. \tag{E.1}$$

For our baseline grid, we set $N = 2$ and $m = 2$.

For x^-, we consider an equal-spaced grid with $sizexm$ points ranging from $min\left(e_1 A\tilde{Z}_t : \tilde{Z} \in grid\right)$ to $max\left(e_1 A\tilde{Z} : \tilde{Z} \in grid\right)$. This choice of grid ensures that the grid for x^- covers the entire range of output gap values implied by the grid for $\tilde{Z}$. In our baseline evaluation, we set $sizexm = 2$.

With $N = 2$ grid points along each of the three dimensions of $\tilde{Z}$, 50 gridpoints for $\hat{s}$, and $sizexm = 2$ grid points for x^-, the combined grid has a total of $2^3 \cdot 50 \cdot 2 \cdot = 800$ points.

E.1.2 Numerical integration

Following Wachter (2005), we use Gauss-Legendre quadrature to evaluate the expectations (D.44), (D.57), and (D.62) numerically. Gauss-Legendre quadrature is orders of magnitude faster than computing expectations by simulation. As in Wachter (2005), we evaluate infinite integrals over the density of standardized consumption shocks ($\epsilon_{1,t}$) using 40 integration node points and an integration domain ranging from -8 standard deviations to $+8$ standard deviations. To conserve speed and memory, we integrate over shocks orthogonal to surplus consumption ($\epsilon_{2,t}$) using a somewhat smaller number of integration node points, 15, but again an integration domain of ± 8 standard deviations. To evaluate bond and stock prices at points that are not on the grid, we use loglinear multi-linear interpolation and extrapolation.

For completeness, we recap the key features of Gauss-Legendre integration. Let $xGL_i,\ i = 1, ..., N_{GL}$ and $wGL_i = 1, ..., N_{GL}$ denote the Gauss-Legendre nodes and weights of N_{GL}th order. Gauss-Legendre quadrature then approximates a definite integral of any smooth function f on the interval $[-1, 1]$ by $\int_{-1}^{1} f(x)\, dx \approx \sum_{i=1}^{N_{GL}} wGL_i f(xGL_i)$. By change of variable, it is immediate that we can approximate the integral of a smooth function f on an interval $[-\bar{a}, \bar{a}]$ by

$$\int_{-\bar{a}}^{\bar{a}} f(x)\, dx \approx \sum_{i=1}^{N_{GL}} \underbrace{\bar{a} \times wGL_i}_{wGL_i^{\bar{a}}} f\left(\underbrace{\bar{a} \times xGL_i}_{xGL_i^{\bar{a}}}\right). \tag{E.2}$$

Here, we use $xGL_i^{\bar{a}}$ and $wGL_i^{\bar{a}}$ to denote Gauss-Legendre node points and weights scaled to the interval $[-\bar{a}, \bar{a}]$.

We implement Gauss-Legendre quadrature to take expectations over ϵ_{t+1} as follows. Let N_1 denote the number of Gauss-Legendre nodes and $\bar{a}_1$ denote the integration domain for the shock $\epsilon_{1,t}$, that is perfectly correlated with output innovations. We set $xGL_{1,i} = xGL_i^{\bar{a}_1}$ and $wGL_{1,i} = wGL_i^{\bar{a}_1}$ for $i = 1, ..., N_1$, where the weights and nodes are as defined in equation (E.2). Moreover, we set

$$pGL_{1,i} = \frac{1}{\sqrt{2\pi}} exp\left(-xGL_{1,i}^2\right) wGL_{1,i} / \sum_{i=1}^{N_1} \left(\frac{1}{\sqrt{2\pi}} exp\left(-xGL_{1,i}^2\right) wGL_{1,i}\right), \tag{E.3}$$

and use the scaled weights $pGL_{1,i}$ for numerical integration. The scaling of (E.3) ensures that the numerical expectation of a constant is evaluated to be the same constant (or intuitively that discretized probabilities sum to one).

We then evaluate numerically the expectation of any smooth function f of $\epsilon_{1,t}$ via:

$$\begin{aligned} E\left[f\left(\epsilon_{1,t}\right)\right] &= \int_{-\infty}^{\infty} \frac{1}{\sqrt{2\pi}} exp\left(-\epsilon_1^2\right) f\left(\epsilon_1\right) d\epsilon_1, & \text{(E.4)} \\ &\approx \int_{-\bar{a}_1}^{\bar{a}_1} \frac{1}{\sqrt{2\pi}} exp\left(-\epsilon_1^2\right) f\left(\epsilon_1\right) d\epsilon_1, & \text{(E.5)} \\ &\approx \sum_{i=1}^{N_1} pGL_{1,i} f\left(xGL_{1,i}\right). & \text{(E.6)} \end{aligned}$$

Accuracy increases with $\bar{a}_1$ and N_1. We follow Wachter (2006) in setting $N_1 = 40$ and $\bar{a}_1 = 8$.

To take expectations over $\epsilon_{2,t}$, we similarly use Gauss-Legendre quadrature with integration domain $\bar{a}_2 = 8$ and number of nodes $N_2 = 15$. We set $xGL_{2,i} = xGL_i^{\bar{a}_2}$ and $wGL_{2,i} = wGL_i^{\bar{a}_2}$ for $i = 1, ..., N_2$ and define the scaled weights:

$$pGL_{2,i} = \frac{1}{\sqrt{2\pi}} exp\left(-xGL_{2,i}^2\right) wGL_{2,i} / \sum_{i=1}^{N_2} \left(\frac{1}{\sqrt{2\pi}} exp\left(-xGL_{2,i}^2\right) wGL_{2,i} \right), \quad \text{(E.7)}$$

Since $\epsilon_{1,t}$ and $\epsilon_{2,t}$ are independent, we can evaluate the expectation of any smooth function $f\left(\epsilon_{1,t}, \epsilon_{2,t}\right)$ as

$$\begin{aligned} Ef\left(\epsilon_{1,t}, \epsilon_{2,t}\right) &= \int_{-\infty}^{\infty} \frac{1}{\sqrt{2\pi}} exp\left(-\epsilon_2^2\right) \int_{-\infty}^{\infty} \frac{1}{\sqrt{2\pi}} exp\left(-\epsilon_1^2\right) f\left(\epsilon_1, \epsilon_2\right) d\epsilon_1 d\epsilon_2, & \text{(E.8)} \\ &\approx \sum_{i=1}^{N_2} pGL_{2,i} \left[\sum_{j=1}^{N_1} pGL_{1,j} f\left(xGL_{1,i}, xGL_{2,j}\right) \right]. & \text{(E.9)} \end{aligned}$$

E.1.3 Recursive step

Let a superscript ^{num} denote the numerical counterparts to the analytic functions f_n, b_n, $b_n^{\$}$. We start by initializing $f_1^{num}\left(\tilde{Z}, \hat{s}, x^-\right)$, $b_2^{num}\left(\tilde{Z}, \hat{s}, x^-\right)$, and $b_2^{\$,num}\left(\tilde{Z}, \hat{s}, x^-\right)$ at each grid point according to the analytic expressions (D.41), (D.53) and (D.55).

Next, we apply the recursive expressions (D.44), (D.57), and (D.62) along the grid. Having computed f_{n-1}^{num} along the entire grid, we evaluate $f_n^{num}\left(\tilde{Z}, \hat{s}, x^-\right)$ at a

grid point $\left(\tilde{Z}, \hat{s}, x^{-}\right)$ as follows. We compute the expectation (D.44) numerically as:

$$\begin{aligned} f_n^{num}(\tilde{Z}, \hat{s}, x^{-}) &= \log\left[\sum_{j=1}^{N2} pGL_{2,j}\left[\sum_{i=1}^{N1} pGL_{1,i}\cdot\exp\Big(g + e_1[B-\phi I]A^{-1}\tilde{Z}\right.\right. \\ &\quad -\bar{r} - (e_3 - e_2 B)A^{-1}\tilde{Z} - \frac{\gamma}{2}(1-\theta_0)(1-2\hat{s}) \\ &\quad -(\gamma(1+\lambda(\hat{s}))-1)\sigma_c \times xGL_{1,i} \\ &\quad \left.\left. + f_{n-1}^{num}\left(\tilde{B}\tilde{Z} + \begin{bmatrix} xGL_{1,i} \\ xGL_{2,j} \\ 0 \end{bmatrix}, \theta_0\hat{s} + \theta_1 x + \theta_2 x^{-} + \lambda(\hat{s})\, xGL_{1,i}, x\right)\right]\right], \end{aligned} \tag{E.10}$$

where we evaluate x as a function of the state vector as

$$x = e_1 A^{-1}\tilde{Z}. \tag{E.11}$$

To compute the right-hand-side of (E.10), we need to evaluate f_{n-1}^{num} at points that are not on our grid. We interpolate f_{n-1}^{num} linearly (and hence F_{n-1}^{num} log-linearly). When the argument is outside the range of the grid, we extrapolate f_{n-1}^{num} linearly. It is clear from (D.41) that linear inter- and extrapolation gives a good approximation of f_1. In fact, we can see that f_1 is exactly linear in $\tilde{Z}$, independent of x^{-}, and that it depends on $\lambda(\hat{s}) = \lambda_0\sqrt{1-2\hat{s}}$. We accommodate the fact that f_1 is not linear in $\hat{s}$ by choosing a much denser grid along the $\hat{s}$ dimension. We do not have analytic expressions for $f_n, n > 1$ (after all, that's why we need a numerical solution), but numerical solutions indicate that linear inter- and extrapolation gives good approximations for f_n with the chosen grid.

In terms of coding (E.10), we face a trade-off between speed and readability of the code. We pre-allocate matrices outside loops and we code linear interpolation by hand (rather than using a pre-written interpolation routine) to conserve speed and memory. We also inline the linear interpolation steps (i.e. write them directly into the main function rather than calling a separate interpolation function). This speeds up the code substantially, while reducing its readability.

There are different methods to interpolate multidimensional functions. Specifically, we use multi-linear interpolation, corresponding to interpolating along each dimension one at a time. In order to enhance computational speed we do not rely on a pre-programmed interpolation routine, instead coding our own minimal interpolation routine. It is well-known that the result of multi-linear (or in the two-dimensional case bi-linear) interpolation does not depend on in which order one interpolates the different arguments. We find it convenient to interpolate $f_{n-1}^{num}\left(\tilde{Z}, \hat{s}, x^{-}\right)$ first along the x^{-} dimension, then along $\hat{s}$, then along $\tilde{Z}_1$, and finally along the $\tilde{Z}_2$ and $\tilde{Z}_3$ dimensions.

Finally, we evaluate the price-consumption ratio for the aggregate consumption stream by approximating it as the sum of the first 300 zero-coupon consumption

claims:

$$G^{num}\left(\tilde{Z}_t, \hat{s}_t, x_{t-1}\right) = \sum_{n=1}^{300} exp\left(f_n^{num}(\tilde{Z}_t, \hat{s}_t, x_{t-1})\right). \tag{E.12}$$

We iterate $b_n^{num}\left(\tilde{Z}, \hat{s}, x^-\right)$ and $b_n^{\$,num}\left(\tilde{Z}, \hat{s}, x^-\right)$ similarly according to:

$$\begin{aligned} b_n^{num}(\tilde{Z}_t, \hat{s}_t, x_{t-1}) = \log\Bigg[\sum_{j=1}^{N2} pGL_{2,j}\Bigg[\sum_{i=1}^{N1} pGL_{1,i} \cdot \exp\Big(&-\bar{r} - (e_3 - e_2 B)\, A^{-1}\tilde{Z} - \frac{\gamma}{2}(1-\theta_0)(1-2\hat{s}) \\ &-\gamma\left(1+\lambda(\hat{s})\right)\sigma_c \times xGL_{1,i} \\ &+b_{n-1}^{num}\left(\tilde{B}\tilde{Z} + \begin{bmatrix} xGL_{1,i} \\ xGL_{2,j} \\ 0 \end{bmatrix}, \theta_0\hat{s} + \theta_1 x + \theta_2 x^- + \lambda\left(\hat{s}\right) xGL_{1,i}, x\right)\Bigg]\Bigg], \end{aligned} \tag{E.13}$$

and

$$\begin{aligned} b_n^{\$,num}(\tilde{Z}_t, \hat{s}_t, x_{t-1}) = \log\Bigg[\sum_{j=1}^{N2} pGL_{2,j}\Bigg[\sum_{i=1}^{N1} pGL_{1,i} \cdot \exp\Big(&-\bar{r} - e_3 A^{-1}\tilde{Z} - \frac{\gamma}{2}(1-\theta_0)(1-2\hat{s}) \\ &-\left(\gamma\left(1+\lambda(\hat{s})\right)\sigma_c + vpi_1 + n \cdot vec^* e_1'\right) \times xGL_{1,i} \\ &-\left(vpi_2 + n \cdot vec^* e_2'\right) xGL_{2,j} + \frac{n^2}{2}\left(\sigma^{\perp}\right)^2 \\ &+b_{n-1}^{\$,num}\left(\tilde{B}\tilde{Z} + \begin{bmatrix} xGL_{1,i} \\ xGL_{2,j} \\ 0 \end{bmatrix}, \theta_0\hat{s} + \theta_1 x + \theta_2 x^- + \lambda\left(\hat{s}\right) xGL_{1,i}, x\right)\Bigg]\Bigg], \end{aligned} \tag{E.14}$$

We again use multi-linear interpolation and extrapolation to evaluate $b_{n-1}^{\$,num}$ and b_{n-1}^{num} at points that are not on the grid.

We similarly implement the recursions (D.95), (D.97), and (D.104) numerically to obtain risk-neutral bond and consumption claim valuations $B_n^{rn,num}$, $B_n^{rn,\$,num}$, $G^{rn,num}$.

E.2 Simulating the Model

We simulate a draw of length T. Reported results in Tables 2 through 5 use $T = 10000$ and discard the first 100 simulation periods to ensure that the system has reached the stochastic steady-state. Tables 2 through 5 report model moments averaged across 2 independent simulations.

We use superscript *sim* to denote simulated quantities. We use the MATLAB function mvnrnd to draw $\epsilon_1^{sim}, ..., \epsilon_T^{sim} \overset{iid}{\sim} N\left(0, diag(1,1,0)\right)$. We similarly generate

independent draws for the orthogonal shock $\epsilon_1^{\perp,sim}, ..., \epsilon_T^{\perp,sim} \overset{iid}{\sim} N(0, \sigma^{\perp})$. We generate draws for u_t^{*sim} by plugging ϵ_t^{sim} and $\epsilon_t^{\perp,sim}$ into (D.60). We generate draws for $\tilde{Z}_t^{sim}, t = 1, ..., T$ by setting $\tilde{Z}_1^{sim} = 0$ and then updating according to (D.30). This gives the simulated output gap, inflation gap, and interest rate gap for $t = 1, 2, ..., T$ through the relation
$\left[x_t^{sim}, \hat{\pi}_t^{sim}, \hat{i}_t^{sim}\right] = \hat{Y}_t^{sim} = A^{-1}\tilde{Z}_t^{sim}$. We generate draws for the surplus consumption ratio by setting $\hat{s}_1^{sim} = 0$ and $x_0^{sim} = 0$ and then updating according to (D.22). We generate the simulated inflation target series $\pi_t^*, t = 1, 2, ..., T$ by starting from $\pi_1^{*sim} = 0$ and updating it according to equation (22) in the main paper. We initialize simulated log consumption at $c_1^{sim} = 0$ and update it using (D.17). We then drop the first 100 simulation periods to allow the system to converge to the stochastic steady-state.

Having generated draws for the five state variables $\tilde{Z}^{sim}$, $\hat{s}^{sim}$, and x_{t-1}^{sim}, we obtain the simulated consumption-claim price-dividend ratio as $(P^c/C)_t^{sim} = G^{num}\left(\tilde{Z}_t^{sim}, \hat{s}_t^{sim}, x_{t-1}^{sim}\right)$, n-period real bond prices as
$P_{n,t}^{sim} = B_n^{num}\left(\tilde{Z}_t^{sim}, \hat{s}_t^{sim}, x_{t-1}^{sim}\right)$, and
$B_{n,t}^{\$,sim} = B_n^{\$,num}\left(\tilde{Z}_t^{sim}, \hat{s}_t^{sim}, x_{t-1}^{sim}\right)$. We obtain the corresponding risk-neutral valuation ratios by plugging into the risk-neutral asset pricing solutions:
$(P^c/C)_t^{rn,sim} = G^{rn,num}\left(\tilde{Z}_t^{sim}, \hat{s}_t^{sim}, x_{t-1}^{sim}\right)$,
$P_{n,t}^{rn,sim} = B_n^{rn,num}\left(\tilde{Z}_t^{sim}, \hat{s}_t^{sim}, x_{t-1}^{sim}\right)$, and
$B_{n,t}^{rn,\$,sim} = B_n^{rn,\$,num}\left(\tilde{Z}_t^{sim}, \hat{s}_t^{sim}, x_{t-1}^{sim}\right)$. We obtain nominal bond prices $P_{n,t}^{\$,sim}$ by combining $B_{n,t}^{\$,sim}$ and π_t^{*sim} according to (D.46). We similarly obtain risk-neutral nominal bond prices $P_{n,t}^{rn,\$,sim}$ by combining $B_{n,t}^{rn,\$,sim}$ and π_t^{*sim} according to (D.46).

To deal with the fact that $\tilde{Z}_t^{sim}$, $\hat{s}_t^{sim}$, x_{t-1}^{sim} are not usually on grid points we adopt a similar linear interpolation strategy as in the numerical evaluation of the asset pricing recursions described in Section E.1.3. We interpolate G^{num}, B_n^{num}, and $B_n^{\$,num}$ log-linearly. We simplify the interpolation strategy slightly compared to Section E.1.3. We use the MATLAB function griddedInterpolant, sacrificing some computational speed for simpler code. Even though rare events (and especially extremely negative realizations for $\hat{s}$) matter for the value function iteration in Section E.1.3, low-probability events have very little impact on the properties of simulated asset prices taking as given G^{num}, B^{num}, and $B^{\$,num}$. We therefore simplify the log-linear interpolation by truncating $\tilde{Z}_t^{sim}$, $\hat{s}_t^{sim}$, and x_{t-1}^{sim} at the maximum and minimum values covered by the grid.

Having generated $\left(\frac{P^c}{C}\right)_t^{sim}, t = 1, ..., T$, we compute log returns on the consumption claim $r_{t+1}^{c,sim}$ according to (D.68). We obtain simulated price-dividend ratios for levered stocks by plugging into (D.75). Finally, we obtain log bond yields and stock and bond excess returns as described in Section D.2.5. Risk-neutral bond and stock

returns are computed by substituting $\left(\frac{P^c}{C}\right)^{rn,sim}$, $P_{n,t}^{rn,\$,sim}$, and $P_{n,t}^{rn,sim}$ into the same relations.

We obtain cash-flow news, real-rate news, and risk-premium excess returns for nominal bonds and levered stocks by substituting simulated returns and real rates into the expression in Section D.3.4. In our simulations, it is possible but very rare (less than 1 in 20000 simulation periods) that the levered price-dividend ratio turns negative. In that event, we discard the simulation run and simulate the model again.

E.3 Parameter units

This subsection details the relation between parameter values in empirical (reported in the paper) and natural units (used for solving the code). We solve the model in natural units. However, it is most natural to report empirical moments and summary statistics in empirical units for interpretability.

For comparability with empirical moments, Table 1 reports model parameters in units that correspond to the output gap in annualized percent, and inflation and interest rates in annualized percent. For comparability with Campbell-Cochrane, we report the discount rate and the persistence of surplus consumption in annualized units. Concretely, Table 1 reports the following scaled parameters:

$$400 \times g, \tag{E.15}$$
$$400 \times \bar{r}, \tag{E.16}$$
$$\theta_0^4, \tag{E.17}$$
$$\beta^4, \tag{E.18}$$
$$\frac{1}{4} \times \psi, \tag{E.19}$$
$$400 \times \sigma_\pi, \tag{E.20}$$
$$400 \times \sigma_i, \tag{E.21}$$
$$400 \times \sigma_*, \tag{E.22}$$
$$4 \times b_{\pi x}, \tag{E.23}$$
$$4 \times b_{ix} \tag{E.24}$$

All other parameters reported in Table 1 do not need to be scaled.

F Details: Econometric methodology

F.1 Impulse response functions

This section describes how we estimate the macroeconomic impulse responses, that we use for the SMM estimation and are shown in Figures 3 through 5. We follow the procedure described below for both actual and simulated data, with the simulated data length matching the length of the empirical sample. Model impulse responses in Figures 3 through 5 are averaged over 100 simulations. In this section, we use subscripts $_{IRF}$ if variable names would otherwise be similar to different variables elsewhere in the paper.

We estimate a VAR(1) of the form

$$Y_{IRF,t} = \Pi Y_{IRF,t-1} + \varepsilon_t, \tag{F.1}$$

where we define the vector for the VAR(1) as:

$$Y_{IRF,t} = [x_{t-1}, \pi_t, i_t]. \tag{F.2}$$

The shocks ε_t are not orthogonal and we denote their estimated variance-covariance matrix by Σ_ε.

Next, we rotate the innovations to be orthogonal. This means that we need to re-write the VAR(1) in the form:

$$R^{-1}Y_{IRF,t} = \Pi_R Y_{IRF,t-1} + \eta_t, \tag{F.3}$$

where η_t is a vector of uncorrelated shocks, R is an invertible matrix, and $\Pi_R = R^{-1}\Pi$. We write the variance-covariance matrix of η_t as:

$$\Sigma_\eta = E\eta_t'\eta_t, \tag{F.4}$$

$$= \begin{bmatrix} \sigma(\eta_1)^2 & 0 & 0 \\ 0 & \sigma(\eta_2)^2 & 0 \\ 0 & 0 & \sigma(\eta_3)^2 \end{bmatrix}. \tag{F.5}$$

There are many ways of writing the VAR(1) in the form (F.3). Following Sims (1986), we pick a unique representation by requiring R^{-1} to be lower-diagonal with ones along the diagonal. Having estimated Π and Σ_ε, we obtain R, Π_R, and Σ_η as follows:

1. Obtain the matrix C_{IRF} as the lower-triangular Cholesky factorization such that $\Sigma_\varepsilon = C_{IRF}C_{IRF}'$ (MATLAB: C=chol(Sigmae,'lower'))

2. Further decompose C_{IRF} into a lower triangular matrix with unit coefficients along the diagonal R and a diagonal matrix D_{IRF}, i.e. $C_{IRF} = RD_{IRF}$, where R has ones along the diagonal and D_{IRF} is a diagonal matrix. (MATLAB: D=diag(diag(C)); $R = C * inv(D)$)

3. We can then multiply (F.1) by R^{-1} to get

$$R^{-1}Y_{IRF,t} = R^{-1}\Pi Y_{IRF,t-1} + R^{-1}\varepsilon_t. \tag{F.6}$$

The variance-covariance matrix of $\eta_t = R^{-1}\varepsilon_t$ is diagonal with

$$\begin{aligned} & E\left[R^{-1}\varepsilon_t\left(R^{-1}\varepsilon_t\right)'\right], && \text{(F.7)}\\ = \; & R^{-1}\Sigma_\varepsilon R^{-1'}, && \text{(F.8)}\\ = \; & R^{-1}C_{IRF}C'_{IRF}R^{-1'}, && \text{(F.9)}\\ = \; & R^{-1}RD_{IRF}D'_{IRF}R'R^{-1'}, && \text{(F.10)}\\ = \; & D_{IRF}D'_{IRF}. && \text{(F.11)} \end{aligned}$$

We therefore define:

$$\begin{aligned} \eta_t &= R^{-1}\varepsilon_t, && \text{(F.12)}\\ \Sigma_\eta &= D_{IRF}D'_{IRF}, && \text{(F.13)}\\ \Pi_R &= R^{-1}\Pi. && \text{(F.14)} \end{aligned}$$

We can now solve for impulse responses. For the output gap impulse responses we start with a unit standard deviation shock to the output gap. We therefore look at macroeconomic impulse responses, where the period 1 shock equals

$$\eta_1 = [\sigma(\eta_1), 0, 0]', \tag{F.15}$$

and shocks in all other periods equal zero. Equivalently, we look at the impulse response to the shock

$$\varepsilon_1 = R[\sigma(\eta_1), 0, 0]', \tag{F.16}$$

and $\varepsilon_t = 0 \; \forall t > 1$. The n response to a one standard deviation shock to the output gap then is computed as:

$$\begin{aligned} & \Pi^{n-1}\varepsilon_1, && \text{(F.17)}\\ = \; & \Pi^{n-1}R\left[\sigma(\eta_1), 0, 0\right]'. && \text{(F.18)} \end{aligned}$$

Impulse responses to inflation and Federal Funds rate shocks are computed analogously as $\Pi^{n-1}R[0, \sigma(\eta_2), 0]'$ and $\Pi^{n-1}R[0, 0, \sigma(\eta_3)]'$.

F.2 Expressions for correlations with the output gap

The SMM estimation procedure matches the correlation between innovations to the 20-quarter expected Federal Funds rate and output gap innovations. In the data, we proxy for this correlation as

$$\widehat{Corr}_{xi} \equiv \widehat{Corr}\left(\frac{1}{20}\left(i_t + i_{t+1} + ... + i_{t+19}\right), x_t\right), \tag{F.19}$$

where t ranges from the first to the last quarter in either period 1 or period 2. The empirical correlation of 5-year average inflation with the output gap is computed analogously, with $i_t, i_{t+1}, .., i_{t+19}$ replaced by π_t, π_{t+1}, $...\pi_{t+19}$. The empirical inflation-output gap correlation is computed as

$$\widehat{Corr}\left(\pi_t, x_t\right), \tag{F.20}$$

where t ranges from the first to the last quarter in either period 1 or period 2.

The model conditional correlation of the 5-year expected Federal Funds rate with the output gap is computed analytically according to:

$$Corr_{t-1}\left(\frac{1}{20}E_t\left(i_t + i_{t+1} + ... + i_{t+19}\right), x_t\right), \tag{F.21}$$

$$= \frac{Q_M\Sigma_u\left(e_3\left(I-B\right)^{-1}\left(I-B^{20}\right)Q + 20e_3\right)'}{\sqrt{Q_M\Sigma_u Q_M'}\sqrt{\left(e_2\left(I-B\right)^{-1}\left(I-B^{20}\right)Q + 20e_3\right)\Sigma_u\left(e_3\left(I-B\right)^{-1}\left(I-B^{20}\right)Q + 20e_3\right)'}}. \tag{F.22}$$

The model conditional correlation of 5-year expected inflation with the output gap equals:

$$Corr_{t-1}\left(\frac{1}{20}E_t\left(\pi_t + \pi_{t+1} + ... + \pi_{t+19}\right), x_t\right), \tag{F.23}$$

$$= \frac{Q_M\Sigma_u\left(e_2\left(I-B\right)^{-1}\left(I-B^{20}\right)Q + 20e_3\right)'}{\sqrt{Q_M\Sigma_u Q_M'}\sqrt{\left(e_2\left(I-B\right)^{-1}\left(I-B^{20}\right)Q + 20e_3\right)\Sigma_u\left(e_3\left(I-B\right)^{-1}\left(I-B^{20}\right)Q + 20e_3\right)'}}. \tag{F.24}$$

The model conditional correlation of one-quarter inflation with the output gap equals:

$$Corr_{t-1}\left(\pi_t, x_t\right) = \frac{Q_M\Sigma_u\left(e_2Q + e_3\right)'}{\sqrt{Q_M\Sigma_u Q_M'}\sqrt{\left(e_2Q + e_3\right)\Sigma_u\left(e_2Q + e_3\right)'}} \tag{F.25}$$

F.3 Confidence intervals and objective function

We use a bootstrap method to compute confidence intervals for the empirical impulse responses shown in Figures 3 through 5 and for the variances of the impulse responses used in the SMM estimation. Let Π and Σ_ε denote the VAR(1) coefficient matrix and the variance-covariance matrix of shocks from estimating (F.1) on actual data. We then generate bootstrapped data from this VAR(1) by simulating $Y^{boot}_{IRF,t}$ of identical sample length as the true data according to

$$Y^{boot}_{IRF,t} = \Pi Y^{boot}_{IRF,t-1} + \varepsilon^{boot}_t, \tag{F.26}$$

where ε^{boot}_t are drawn as iid normal with mean zero and variance-covariance Σ_ε. On the bootstrapped data, we then apply the methodology for IRFs described in Section F.1. That is, we re-estimate (F.1) on the bootstrapped data and use the resulting estimates to construct bootstrapped impulse response functions. We generate 1000 independent bootstrap samples. Figures 3 through 5 show confidence intervals, such that 95% of the time the bootstrapped impulse responses are within the interval.

For our objective function, we define the empirical target moments as follows. $\hat{\Psi}$ is $[52 \times 1]$. It includes $51 = 6 \cdot 9 - 3$ impulse responses and the 5-year average Federal Funds rate-output gap correlation. We have 51 impulse response moments, because we have nine impulse responses at one (shock period), two, four, 12, 20, and 40 quarters each. However, three of the shock period impulse responses are zero by our choice of orthogonalization and we exclude them from the objective function. The last element of $\hat{\Psi} - \Psi(param)$ is the square-root of the 20-quarter Federal Funds rate-output gap correlation in the model minus the data, defined as

$$\sqrt{\left| Corr_{t-1}\left((i_t + i + t + 1 + ... + i_{19}), x_t \right) - \widehat{Corr}\left(\tfrac{1}{20} (i_t + i + t + 1 + ... + i_{19}), x_t \right) \right|}.$$

Let $\hat{V}$ denote the bootstrapped variance-covariance matrix of $\hat{\Psi}^{boot} - \hat{\Psi}$, where the 51 first elements of $\hat{\Psi}^{boot} - \hat{\Psi}$ are the difference between the bootstrapped impulse response moments and the data impulse responses and the last element is $\sqrt{\widehat{Corr}^{boot}_{xi} - \widehat{Corr}_{xi}}$ and $\widehat{Corr}_{xi}$ and $\widehat{Corr}^{boot}_{xi}$ denote the 5-year average Federal Funds rate-output gap correlation computed according to (F.19) in actual and bootstrapped data. We then define the weighting matrix $\hat{W}$ for the SMM objective function as the diagonal matrix with the inverse variances for the 51 impulse response moments and 200 along the diagonal:

$$\hat{W} = diag(inv(\hat{V}_{1,1}), inv(\hat{V}_{2,2}), ..., inv(\hat{V}_{51,51}), 200). \tag{F.27}$$

F.4 Grid search

We minimize the SMM objective function by grid search. Solving for the macroeconomic dynamics once and simulating the macroeconomic impulse response functions

(but not solving for asset prices) takes about 0.1 seconds. So the reason that the estimation is computationally intensive is that we have a high-dimensional parameter space, combined with the need to simulate impulse responses to adjust for small sample effects in plausibly short empirical samples. We are minimizing over 12 parameters, so we have a high-dimensional optimization problem, for which gradient-based optimization methods do not work well. We solve the challenges posed by high-dimensional optimization by a) dividing parameters into blocks b) using the Harvard Odyssey computing cluster c) grid search along an appropriate grid.

We minimize $Obj(params)$ using a two-step grid search. To reduce the dimensionality of the grid search, we separate the parameters into those determining the slope coefficients in the VAR(1) $params_{slope} = [b_{\pi i}, b_{\pi\pi}, b_{\pi i}, b_{ix}, b_{i\pi}, b_{ii}]$ and those determining the shock variances and correlations
$params_{shocks} = [\sigma_\pi, \sigma_i, \sigma_*, \rho_{\pi i}, \rho_{\pi *}, \rho_{i*}]$. The grid search finds the parameter values for $params_{slope}$ that minimize the objective function while holding the shock parameters at $params_{vol} = [0.1, 0.1, 0.1, 0, 0, 0]$. This first grid search step solves and simulates macroeconomic dynamics over a grid. The grid for this first step consists of 10 equally-spaced points between -1 and 1 for every parameter in $params_{slope}$. In this first step, we thus solve and simulate the macroeconomic dynamics 10^6 times. We discard parameter values in this step, where asset prices do not exist. We achieve this high number of model evaluations by running up to 1000 model simulations in parallel on the Harvard Odyssey computing cluster. In a second step, we find the parameter vector $params_{vol}$ that minimize the objective function while holding constant $params_{slope}$ at the previously estimated values. We use a grid with 10 points for each of the 6 parameters in $params_{slope}$. For the volatilities, we use equal-spaced grids from 0.01% to 0.3%. For the correlations, we use equal-spaced grids from -0.99 to 0.99. We discard parameter vectors where asset prices do not exist.

F.5 Standard errors and hypothesis tests

F.5.1 Standard errors

This Section provides details on the parameter standard errors in Table 1. Despite our non-standard weighting matrix, we can compute standard errors using standard methods, similarly to Bekaert and Engstrom (2017) and CEE. Under the usual conditions, the asymptotic distribution of the parameter estimates $\widehat{params}$ around their true values $params$ is given by:

$$\left(\widehat{params} - params\right) \sim N\left(0, \hat{V}_{params}\right), \tag{F.28}$$

$$\hat{V}_{params} = \left(\hat{M}_{SE}^{-1}\hat{H}_{SE}'\hat{W}\hat{V}\hat{W}\hat{H}_{SE}\hat{M}_{SE}^{-1}\right) \tag{F.29}$$

$\hat{W}$ is the diagonal weighting matrix used in the SMM objective function. $\hat{V}$ is the variance-covariance matrix of empirical moments. Both $\hat{V}$ and $\hat{W}$ are obtained as

described in Section F.3. The matrix $\hat{H}_{SE} = \nabla\Psi\left(\widehat{params}\right)$ is the Jacobian of the model moments evaluated at the vector of point estimates, $\widehat{params}$. Finally, $\hat{M}_{SE} \equiv \hat{H}'_{SE}\hat{W}\hat{H}_{SE}$.

We obtain the i'th column of $\hat{H}_{SE}$ as the numerical derivative of the model moments with respect to parameter i. Specifically, we simulate moments while moving parameter i by $\pm eps_i$ from its point estimate, and dividing the difference by $2eps_i$. We then compute $\hat{H}_{SE}$ according to:

$$\hat{H}_{SE} \;=\; \left[\; \frac{\Psi\left(\widehat{params}+e_1 eps_1\right)-\Psi\left(\widehat{params}-e_1 eps_1\right)}{2eps_1},\;\; \ldots,\;\; \frac{\Psi\left(\widehat{params}+e_{12} eps_{12}\right)-\Psi\left(\widehat{params}-e_{12} eps_{12}\right)}{2eps_{12}} \;\right]. \tag{F.30}$$

The matrix $\hat{H}_{SE}$ is $[52 \times 12]$, because we have 52 moments and 12 parameters.

There are two practical challenges when computing standard errors. The first one is that the 12×12 matrix $\hat{M}_{SE}$ may be hard to invert if its eigenvalues have drastically different orders of magnitude. We deal with this first challenge by scaling the standard deviations by 400 before doing the standard errors calculation. The second challenge is that our moments are simulated, so there is simulation noise around the true $\Psi\left(\widehat{params} \pm e_i eps_i\right)$. We deal with this second challenge by choosing values for eps_i that are large enough that movements in model moments are not dominated by simulation noise. We allow for different epsilons eps_i for different parameters, because parameters have different scales. Specifically, we set $eps_i = 0.25 \times \left|\widehat{params}_i\right|$.

F.5.2 Hypothesis tests

Let $\widehat{params}_1$ and $\widehat{params}_2$ denote the parameter point estimates for periods 1 and 2. Let $\hat{V}_{params,1}$ and $\hat{V}_{params,2}$ denote the asymptotic variance-covariance matrices for periods 1 and 2, as defined in equation (F.29).

Table 1 reports the results from testing whether parameter i is equal in periods 1 and 2. Under the null hypothesis that $params_1(i) = params_2(i)$, we have that:

$$\widehat{params}_2(i) - \widehat{params}_1(i) \;\sim\; N\left(0, e_i\left(V_{params,1} + \hat{V}_{params,2}\right)e_i'\right). \tag{F.31}$$

The test statistic is:

$$\left(\widehat{params}_2(i) - \widehat{params}_1(i)\right)\left(e_i\left(\hat{V}_{params,1} + \hat{V}_{params,2}\right)e_i'\right)^{-1}\left(\widehat{params}_2(i) - \widehat{params}_1(i)\right) \;\sim\; \chi^2_1. \tag{F.32}$$

We compute p-value for the test that $params_1(i) = params_2(i)$ by plugging the test statistic (F.32) into the CDF of a chi-squared distribution with 1 degree of freedom.

F.6 Kalman filter for Figure 1

In this section, we use subscript $_{kal}$ to denote parameters and processes specific to the Kalman filter to distinguish them from variables with similar names elsewhere in the paper. Let β_t denote the bond beta estimated from daily returns over the past quarter t. We model β_t as an unobserved AR(1) component plus white measurement noise. We denote the deviation of β_t from its mean μ_{kal} by:

$$y_{kal,t} = \beta_t - \mu_{kal}. \tag{F.33}$$

We assume that $y_{kal,t}$ satisfies the plant and observation equations:

$$x_{kal,t} = A_{kal} x_{kal,t-1} + u_{kal,t}, \tag{F.34}$$

$$y_{kal,t} = x_{kal,t} + v_{kal,t}, \tag{F.35}$$

where $u_{kal,t}$ and $v_{kal,t}$ are mean zero, independent random variables with variances $\sigma^2_{kal,u}$ and $\sigma^2_{kal,v}$. The unobserved component $x_{kal,t}$ is the latent de-meaned beta of nominal bonds, that we want to estimate.

We can re-write the system (F.34) and (F.35) as:

$$x_{kal,t} = A_{kal} x_{kal,t-1} + \epsilon_{kal,t}, \tag{F.36}$$

$$y_{kal,t} = C_{kal} x_{kal,t-1} + \eta_{kal,t}, \tag{F.37}$$

where

$$C_{kal} = A_{kal}, \tag{F.38}$$

$$N_{kal} = Var(\epsilon_{kal,t}) = \sigma^2_{kal,u}, \tag{F.39}$$

$$L_{kal} = Cov(\epsilon_{kal,t}, \eta_{kal,t}) = \sigma^2_{kal,u}, \tag{F.40}$$

$$M_{kal} = Var(\eta_{kal,t}) = \sigma^2_{kal,u} + \sigma^2_{kal,v}. \tag{F.41}$$

Let $W_{kal,t}$ denote the information available up to time t from observing ..., β_{t-1}, β_t. Suppose that conditional on $W_{kal,0}$ the initial state $x_{kal,0}$ is distributed $N(\hat{x}_{kal,0}, V_{kal,0})$ and the state and observations obey the recursions (F.36) through (F.37). Standard Kalman filter results then imply that conditional on $W_{kal,t}$, the current state is distributed $N(\hat{x}_{kal,t}, V_{kal,t})$ and that the conditional mean and variance obey the updating recursions:[3]

$$\hat{x}_{kal,t} = A_{kal}\hat{x}_{kal,t-1} + H_{kal,t}(y_{kal,t} - C_{kal}\hat{x}_{kal,t-1}), \tag{F.42}$$

$$\begin{aligned} V_{kal,t} = {} & N_{kal} + A_{kal} V_{kal,t-1} A'_{kal} \\ & -(L_{kal} + A_{kal} V_{kal,t-1} C'_{kal}) \cdot \\ & (M_{kal} + C_{kal} V_{kal,t-1} C'_{kal})^{-1} (L'_{kal} + C_{kal} V_{kal,t-1} A'_{kal}), \end{aligned} \tag{F.43}$$

$$H_{kal,t} = (L_{kal} + A_{kal} V_{kal,t-1} C'_{kal})(M_{kal} + C_{kal} V_{kal,t-1} C'_{kal})^{-1}. \tag{F.44}$$

[3]We substitute into the Kalman filter updating equations from Richard Weber's Optimization and Control class notes available at http://www.statslab.cam.ac.uk/ rrw1/oc/index.html.

The distribution of $y_{kal,t}$ conditional on the information available at time $t-1$ is normal with conditional mean:

$$E(y_{kal,t}|W_{kal,t-1}) \;=\; C_{kal}\hat{x}_{kal,t-1}, \tag{F.45}$$

and variance

$$Var(y_{kal,t}|W_{kal,t-1}) \;=\; M_{kal} + C_{kal}V_{kal,t-1}C'_{kal}. \tag{F.46}$$

The log-likelihood hence obeys the recursion:

$$\begin{aligned} LL(y_{kal,1}, y_{kal,2}, ..., y_{kal,t}) \;=\; & LL(y_{kal,1}, y_{kal,2}, ..., y_{kal,t-1}) \\ & -\frac{1}{2}log(2\pi) - \frac{1}{2}log\left(M_{kal} + C_{kal}V_{kal,t-1}C'_{kal}\right) \\ & -\frac{(y_{kal,t} - C_{kal}\hat{x}_{kal,t-1})^2}{2(M_{kal} + C_{kal}V_{kal,t-1}C'_{kal})}. \end{aligned} \tag{F.47}$$

We estimate the parameters μ_{kal}, A_{kal}, $\sigma_{kal,u}$, $\sigma_{kal,v}$ by maximizing the likelihood function (F.47).

We consider a 95% confidence interval for the unobserved bond beta $x_{kal,t} + \mu_{kal}$ conditional on $W_{kal,t}$:

$$CI(x_{kal,t}|W_{kal,t}) = \left[\hat{x}_{kal,t} + \mu_{kal} - 1.96\sqrt{V_{kal,t}}, \hat{x}_{kal,t} + \mu_{kal} + 1.96\sqrt{V_{kal,t}}\right]. \tag{F.48}$$

The estimated parameters for the betas are as follows: $\mu_{kal} = 0.60$, $A_{kal} = 0.96$, $\sigma_{kalmna,u} = 0.04$, $\sigma_{kal} = 0.08$. We run exactly the same Kalman filter for the quarter-end bond-stock correlations of daily returns and obtain: $\mu_{kal,corr} = 0.08$, $A_{kal,corr} = 0.95$, $\sigma_{kal,corr,u} = 0.10$, $\sigma_{kal,corr,v} = 0.17$. These parameter estimates show that both betas and correlations are estimated to have substantial persistence, but also a high volatility of iid noise, so filtering is useful in filtering out the noise.

G Additional Model Results

G.1 Additional Model Moments

Table G.1: Macroeconomic Dynamics

	79Q3-01Q1		01Q2-11Q4	
	Empirical	Model	Empirical	Model
Nominal Short Rate Changes				
Volatility	1.94	0.86	0.53	0.37
AR(1) Coefficient	-0.36	-0.03	0.60	-0.10
Inflation Changes				
Volatility (%)	0.83	0.96	1.03	1.28
AR(1) Coefficient	-0.27	-0.06	-0.40	-0.26
Consumption growth				
Volatility (%)	0.90	1.75	0.90	1.59
AR(1) Coefficient	0.21	0.03	0.60	0.25
Output gap				
Volatility (%)	1.93	2.09	2.04	5.46
AR(1) Coefficient	0.92	0.91	0.94	0.99

The empirical nominal rate change equals the one-quarter change in the log end-of-quarter Federal Funds rate from the Federal Reserve's H.15 publication. The log Federal Funds rate is averaged over the last five business days of each quarter and expressed in annualized percent. The inflation change equals the one-quarter change in log quarterly inflation. Log quarterly inflation is the log change in the seasonally adjusted GDP deflator in annualized percent. Log real quarterly consumption growth and the log real output gap are in percent. The standard deviation of consumption growth is annualized. We use real consumption expenditures data for nondurables and services from the Bureau of Economic Analysis National Income and Product Accounts Tables. The output gap is log real seasonally adjusted GDP minus log potential real GDP from the Congressional Budget Office. Consumption, the GDP deflator, and real output variables are in chained 2009 dollars and obtained via the St. Louis FRED. Model moments are averaged over 2 simulations of length 10000.

Table G.1 shows that the model generates a low volatility of consumption growth, that is somewhat positively serially correlated. The volatility of nominal short rate changes decreases from period 1 to period 2, just as in the data. The output gap volatility of 5.46% in period 2 might at first appear high. However, we are not concerned about this number because the output gap is also extremely persistent in this period and the volatility of a highly persistent series from a long simulation is hard to compare with a finite-sample volatility in the data. Notably, consumption growth, which is a change and hence not extremely persistent, is not excessively volatile in the model for this period.

Table G.2: Real Bonds

	79Q3-01Q1	01Q2-11Q4
Excess Returns		
Term Premium	1.41	-0.94
Volatility	2.97	2.05
Sharpe Ratio	0.48	-0.46
Yields		
Mean log Yield Spread	0.77	-0.44
Volatility	1.15	0.55
Bond-Stock Comovement		
Bond-Stock Beta	0.13	-0.11
Bond-Stock Correlation	0.96	-0.88

This table reports model moments for 5-year real zero coupon bonds. The quarterly 5-year real bond excess return is defined as the quarterly log return on a 5-year real zero-coupon bond in excess of the 3-month log real risk-free rate. All moments for real bonds are computed analogously to nominal bond moments in Table 3 in the main paper. The term premium, volatility of real bond excess returns, and the log yield spread are in annualized percent. Model moments are averaged over 2 simulations of length 10000.

Table G.2 shows model implications for real bonds. Model-implied real bond-stock return correlations changed from positive in period 1 to negative in period 2. US inflation-indexed bonds (TIPS) only became available during the second half of our sample and even then remained illiquid. With this caveat, the model real bond beta is in line with the data. In period 2, the stock market beta of empirical quarterly log TIPS excess returns was -0.08 in the data, compared to -0.11 in the model.[4] The empirical correlation between log TIPS excess returns and stock returns was large and negative at -0.33, compared to -0.88 in the model. The direction of change in the model-implied real bond-stock correlation is also empirically plausible. US inflation-indexed bonds were not available in our first period, but UK inflation-indexed bonds were. Campbell, Shiller, and Viceira (2009) show that the UK inflation-indexed bond-stock correlation was positive before 2000 and became negative thereafter, similarly to the change implied by our model.

Table G.3 is analogous to Table 5 in the main paper, but it shows correlations rather than covariances.

[4]We measure the quarterly log TIPS excess return as $-(n-1)y_{n,t+1}+ny_{n,t}-i_t+\pi_{t+1}$, where $y_{n,t}$ is measured as the five year continuously compounded TIPS yield. We obtain 5-year TIPS yields from Bloomberg ticker "USGGT05Y Index".

Table G.3: Decomposing Model Bond and Stock Return Correlations

Panel A: Stock Returns

	79Q3-01Q1				01Q2-11Q4			
	Cash Flow	Real Rate	Risk Premium	Total	Cash Flow	Real Rate	Risk Premium	Total
Cash Flow	1.00	0.92	0.93	0.96	1.00	-0.99	0.92	0.94
Real Rate	·	1.00	0.92	0.94	·	1.00	-0.90	-0.91
Risk Premium	·	·	1.00	1.00	·	·	1.00	1.00
Total	·	·	·	1.00	·	·	·	1.00

Panel B: Bond Returns

	79Q3-01Q1				01Q2-11Q4			
	Cash Flow	Real Rate	Risk Premium	Total	Cash Flow	Real Rate	Risk Premium	Total
Cash Flow	1.0	-0.11	0.01	0.86	1.00	-0.32	0.07	0.80
Real Rate	·	1.00	0.83	0.41	·	1.00	0.76	0.29
Risk Premium	·	·	1.00	0.48	·	·	1.00	0.60
Total	·	·	·	1.00	·	·	·	1.00

Panel C: Bond-Stock Returns

	79Q3-01Q1				01Q2-11Q4			
Bonds ↓/Stocks →	Cash Flow	Real Rate	Risk Premium	Total	Cash Flow	Real Rate	Risk Premium	Total
Cash Flow	0.06	-0.08	0.01	0.01	0.04	-0.16	-0.09	-0.12
Real Rate	0.90	0.98	0.88	0.91	-0.92	0.95	-0.81	-0.81
Risk Premium	0.88	0.86	0.97	0.96	-0.87	0.85	-0.95	-0.94
Total	0.53	0.43	0.49	0.50	-0.54	0.44	-0.63	-0.66

This table is analogous to Table 5 in the main paper, but it shows correlations instead of covariances. We decompose model stock and nominal bond returns into real cash flow news, real rate news, and risk premium excess returns (Campbell and Ammer 1993). We solve for risk-neutral bond and stock returns with the risk-neutral pricing kernel $M^{rn}_{t+1} = exp(-r_t)$. We use the loglinear approximation of Campbell and Shiller (1988) to compute real rate news for model stock and bond returns. Cash flow news are computed as risk-neutral excess returns minus real rate news. Risk premium excess returns are the difference between stock or bond log excess returns and risk neutral log excess returns. For details of this decomposition see the appendix. Panel A shows the correlations of stock return real cash flow news, real rate news, risk premium news, and total stock returns. Panel B shows the correlations of bond return real cash flow news, real rate news, risk premium news, and total bond returns. Panel C shows the correlations between bond real cash flow news, real rate news, risk premium news and total bond returns with stock real cash flow news, real rate news, risk premium news, and total stock returns. Model moments are averaged over 2 simulations of length 10000.

G.2 Switching off the new parameters θ_1 and θ_2

This section shows that the new parameters θ_1 and θ_2 are needed to match the macroeconomic impulse responses. To this end, we estimate the model while constraining the new preference parameters θ_1 and θ_2 to equal zero. With $\theta_1 = \theta_2 = 0$, agents have exactly the same preferences as in Campbell and Cochrane (1999). Equation (13) in the main paper shows that when $\theta_1 = \theta_2 = 0$, the macroeconomic Euler equation only has a forward-looking term and no backward-looking term. Macroeconomic models without asset prices, such as Fuhrer (2000) and Christiano, Eichenbaum, and Evans (2005), use preferences that generate a macroeconomic Euler equation with both backward- and forward-looking terms (typically with an approximation). The reason given in those papers for needing a backward-looking term in the Euler equation is that it generates hump-shaped impulse responses to an interest rate shock.

To give our model the best shot at matching the macroeconomic impulse responses with $\theta_1 = \theta_2 = 0$, we re-optimize over the estimated parameters. That is, we set $\theta_1 = \theta_2 = 0$ and re-run the same grid search procedure as for our baseline preference parameters.

Table G.4: Parameters

Panel A: Calibrated Parameters conditional on θ_1 and θ_2 equal 0		
Consumption Growth Rate	g	1.89
Utility Curvature	γ	2.00
Steady-State Riskfree Rate	$\bar{r}$	0.94
Persistence Surplus Cons.	θ_0	0.87
Dependence Output Gap	θ_1	0
Dependence Lagged Output Gap	θ_2	0
Smoothing Parameter Consumption	ϕ	0.93
Leverage	δ	0.50
Implied Parameters		
Discount Rate	β	0.90
Euler Eqn. Lag Coefficient	ρ^x	0
Euler Eqn. Forward Coefficient	f^x	1.08
Euler Eqn. Real Rate Slope	ψ	0.13

Table G.4: Parameters (continued)

Panel B: Estimated Parameters conditional on θ_1 and θ_2 equal 0			
Lag Parameters		79Q3-01Q1	01Q2-11Q4
Inflation-Output Gap	$b_{\pi x}$	0.44	-0.44
Inflation-Inflation	$b_{\pi\pi}$	1.00	1.00
Inflation-Fed Funds	$b_{\pi i}$	0.56	1.00
Fed Funds-Output Gap	b_{ix}	-0.44	-0.44
Fed Funds-Inflation	$b_{i\pi}$	0.78	1.00
Fed Funds-Fed Funds	b_{ii}	0.11	1.00
Std. Shocks (%)			
Std. Infl.	σ_π	0.43	0.56
Std. Fed Funds	σ_i	0.68	0.43
Std. Infl. Unit Root	σ_*	0.43	0.30
Shock Correlations			
Inflation-Fed Funds	$\rho_{\pi i}$	-0.33	-0.11
Inflation-Infl. Unit Root	$\rho_{\pi *}$	-0.11	0.33
Fed Funds-Infl. Unit Root	ρ_{i*}	0.11	-0.33
Implied Parameters			
Steady-State Surplus Cons. Ratio	$\bar{S}$	0.07	0.06
Max. Surplus Cons. Ratio	s_{max}	0.11	0.10

This table is constructed analogously to Table 1 in the main paper, except that the calibrated preference parameters θ_1 and θ_2 are set to zero. Panel A shows calibrated parameters, that are held constant across subperiods. Consumption growth and the steady-state risk-free rate are in annualized percent. The discount rate and the persistence of surplus consumption are annualized. The estimated macroeconomic parameters in Panel B are reported in units corresponding to our empirical variables, i.e. the output gap is in percent, and inflation, the Fed Funds rate and the unit root component of inflation are in annualized percent. The implied Euler equation real rate slope is reported in the same units, that is $\frac{1}{4}\frac{1}{\gamma(\phi-\theta_1)}$. We report quarterly standard deviations of shocks to annualized percent inflation, Fed Funds rate, and inflation target. We use superscripts *,**, and *** to denote that for a parameter we can reject that it is constant across subperiods at the 10%, 5%, and 1% levels, accounting for estimation uncertainty in both periods.

Table G.4 shows the calibrated and estimated parameter values for the estimation with $\theta_1 = \theta_2 = 0$. Table G.4, Panel B shows that many of the estimated parameters are different from the values shown in Table 1 in the main paper. These changes may be due to the inability of the model to fit impulse responses to interest rate innovations with $\theta_1 = \theta_2 = 0$, which distorts estimates of other parameters.

Figure G.2: Impulse Responses to Output Gap Innovations conditional on θ_1 and θ_2 equal 0

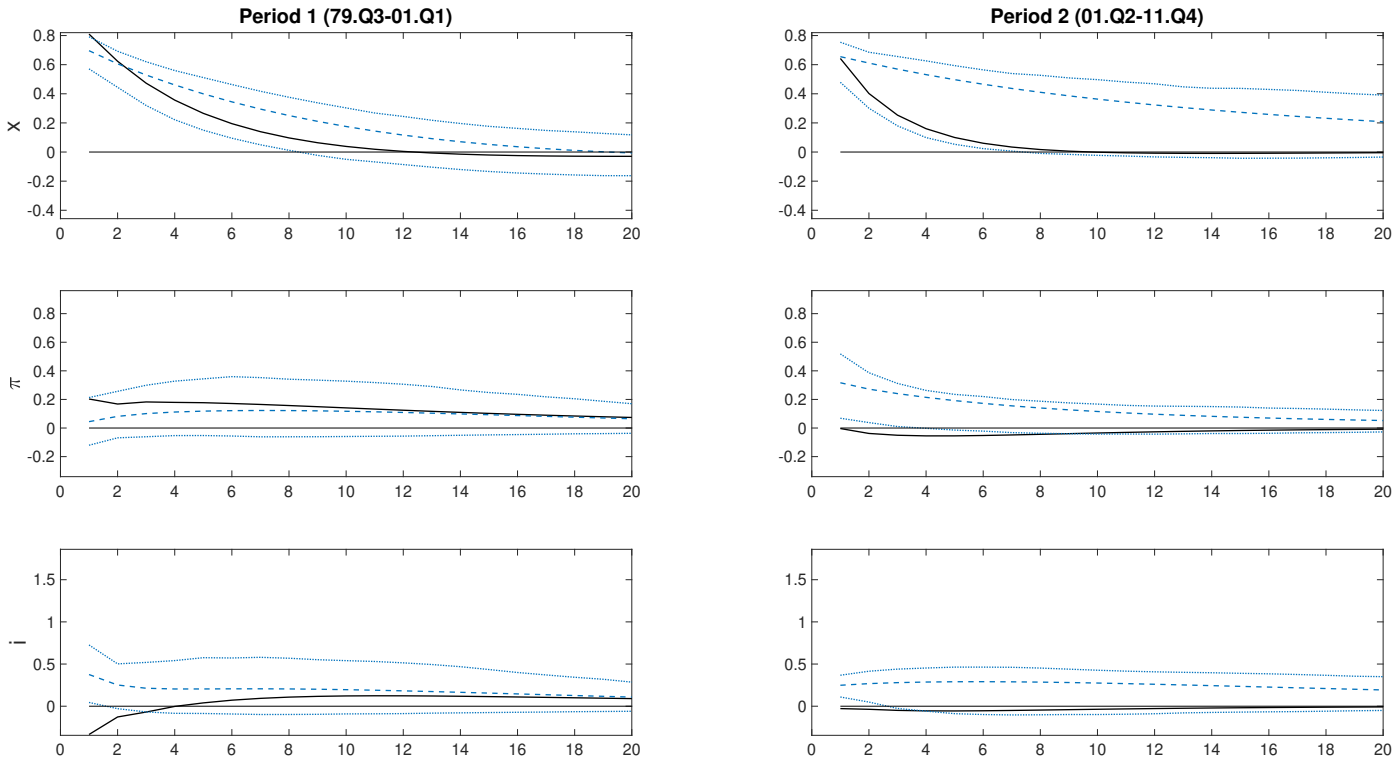

This figure is analogous to Figure 3 in the main paper, but is based on the parameter values shown in Table G.4. This figure shows model (black) and data (blue with 95% CI) orthogonalized impulse responses for the output gap, inflation, and the Federal Funds rate in response to a one-standard deviation output gap innovation. To provide a unique rotation of impulse responses, shocks are ordered such that an output gap shock affects inflation and the Fed Funds rate contemporaneously, an inflation shock affects the Fed Funds rate but not the output gap contemporaneously, and a Fed Funds rate shock affects neither inflation nor the output gap contemporaneously.

Figure G.3: Impulse Responses to Inflation Innovations conditional on θ_1 and θ_2 equal 0

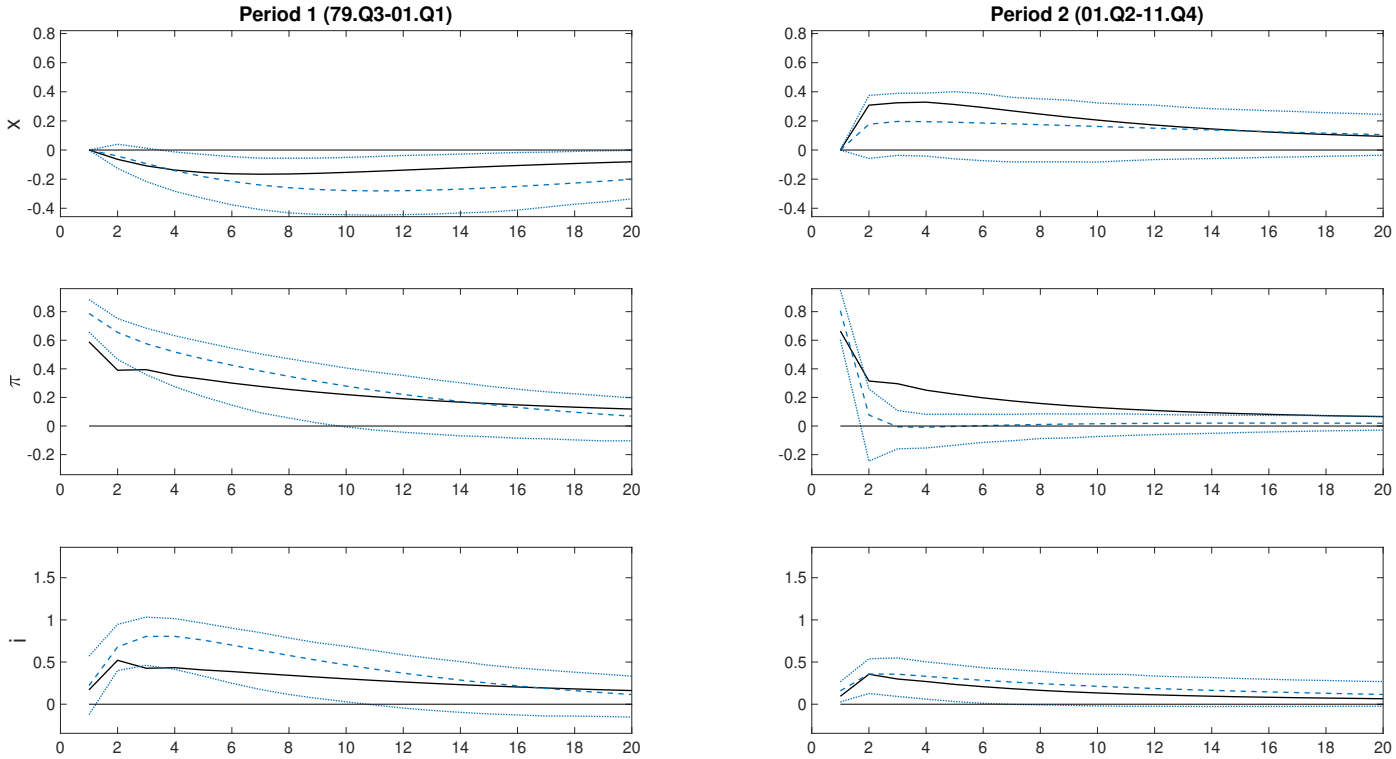

This figure is analogous to Figure 4 in the main paper, but is based on the parameter values shown in Table G.4. This figure shows model (black) and data (blue with 95% CI) orthogonalized impulse responses for the output gap, inflation, and the Federal Funds rate in response to a one-standard deviation inflation innovation. To provide a unique rotation of impulse responses, shocks are ordered such that an output gap shock affects inflation and the Fed Funds rate contemporaneously, an inflation shock affects the Fed Funds rate but not the output gap contemporaneously, and a Fed Funds rate shock affects neither inflation nor the output gap contemporaneously.

Figure G.4: Impulse Responses to Fed Funds Innovation conditional on θ_1 and θ_2 equal 0

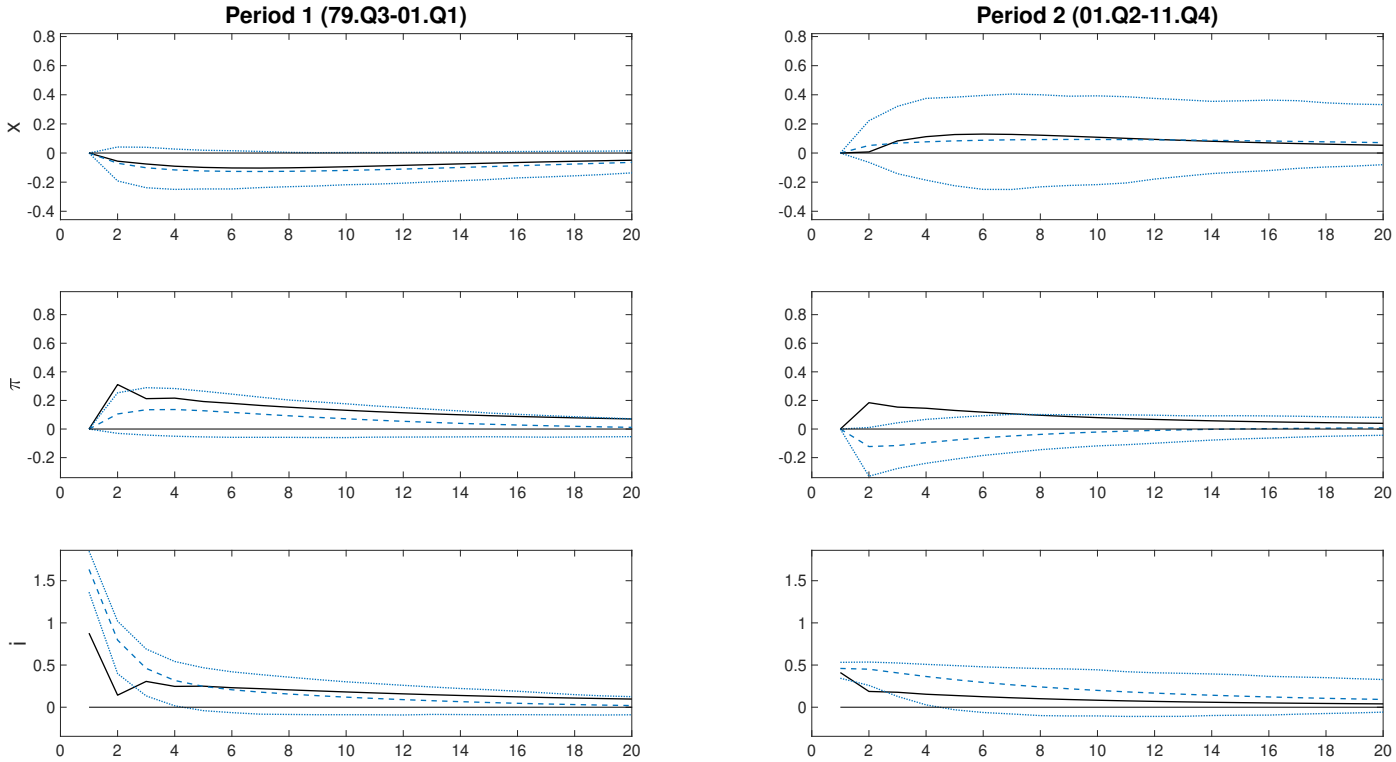

This figure is analogous to Figure 5 in the main paper, but uses the parameter values shown in Table G.4. This figure shows model (black) and data (blue with 95% CI) orthogonalized impulse responses for the output gap, inflation, and the Federal Funds rate in response to a one-standard deviation Federal Funds rate innovation. To provide a unique rotation of impulse responses, shocks are ordered such that an output gap shock affects inflation and the Fed Funds rate contemporaneously, an inflation shock affects the Fed Funds rate but not the output gap contemporaneously, and a Fed Funds rate shock affects neither inflation nor the output gap contemporaneously.

Figures G.2 through G.4 show that the model with $\theta_1 = \theta_2 = 0$ provides an unacceptable fit to the macroeconomic dynamics. The worse model fit with $\theta_1 = \theta_2 = 0$ is particularly apparent in Figure G.4 compared to Figure 5 in the main paper. Figure G.4 shows spikes in inflation, that subsequently mean-revert, in contrast to the smooth and hump-shaped response in the data. Moreover, the inflation response to an interest rate innovation has the wrong sign in Figure G.4. By comparison, Figures 3 through 5 in the main paper generate hump-shaped and smooth impulse responses without spikes for all response variables, and the inflation responses to an interest rate innovation match the sign in the data.

References

Blanchard, Olivier Jean, and Charles M. Kahn, 1980, "The Solution of Linear Difference Models under Rational Expectations", *Econometrica*, 1305–1311.

Campbell, John Y. and John Ammer, 1993, "What Moves the Stock and Bond Markets? A Variance Decomposition for Long-Term Asset Returns", *Journal of Finance* 48, 3–37.

Campbell, John Y. and John H. Cochrane, 1999, "By Force of Habit: A Consumption-Based Explanation of Aggregate Stock Market Behavior", *Journal of Political Economy* 107, 205–251.

Campbell, John Y., Carolin E. Pflueger, and Luis M. Viceira, 2019, "Macroeconomic Policy Drivers of Bond and Equity Risks", working paper, Harvard University and University of British Columbia.

Campbell, John Y., and Robert Shiller, 1988, "The Dividend-Price Ratio and Expectations of Future Dividends and Discount Factors", *Review of Financial Studies* 1(8), 195–228.

Chen, Andrew Y., 2017, "External Habit in a Production Economy: A Model of Asset Prices and Consumption Volatility Risk", *Review of Financial Studies* 30(8) 2890–2932.

Christiano, Lawrence J., Martin Eichenbaum, and Charles L. Evans, 2005, "Nominal Rigidities and the Dynamic Effects of a Shock to Monetary Policy", *Journal of Political Economy* 113, 1–45.

Dai, Qiang, and Kenneth J. Singleton, 2000, "Specification Analysis of Affine Term Structure Models", *Journal of Finance* 55(5), 1943–1978.

Fuhrer, Jeffrey C., 2000, "Habit Formation in Consumption and Its Implications for Monetary-Policy Models", *American Economic Review* 90, 367–390.

Lopez, Pierlauro, J. David López-Salido, and Francisco Vazquez-Grande, 2015, "Macro-Finance Separation by Force of Habit", unpublished paper, Federal Reserve Board and Banque de France.

Rudebusch, Glenn D. and Eric T. Swanson, 2008, "Examining the Bond Premium Puzzle with a DSGE Model", *Journal of Monetary Economics* 55, 111–126.

Uhlig, Harald, 1999, "A Toolkit for Analyzing Nonlinear Dynamic Stochastic Models Easily", in Ramon Marimon and Andrew Scott (eds.) *Computational Methods for the Study of Dynamic Economies*, 30–61, Oxford University Press.

Wachter, Jessica A., 2005, "Solving Models with External Habit", *Finance Research Letters* 2, 210–226.